Development 140, 2082-2092 (2013) doi:10.1242/dev.088203

Ephrin B1 maintains apical adhesion of neural progenitors

Dina N. Arvanitis[1,2], Annie Béhar[1,2], Petra Tryoen-Tóth[3], Jeff O. Bush[4], Thomas Jungas[1,2], Nicolas Vitale[3] and Alice Davy[1,2,*]

SUMMARY

Apical neural progenitors are polarized cells for which the apical membrane is the site of cell-cell and cell-extracellular matrix adhesion events that are essential for maintaining the integrity of the developing neuroepithelium. Apical adhesion is important for several aspects of the nervous system development, including morphogenesis and neurogenesis, yet the mechanisms underlying its regulation remain poorly understood. Here, we show that ephrin B1, a cell surface protein that engages in cell signaling upon binding cognate Eph receptors, controls normal morphogenesis of the developing cortex. *Efnb1*-deficient embryos exhibit morphological alterations of the neuroepithelium that correlate with neural tube closure defects. Using loss-of-function experiments by *ex vivo* electroporation, we demonstrate that ephrin B1 is required in apical progenitors (APs) to maintain their apical adhesion. Mechanistically, we show that ephrin B1 controls cell-ECM adhesion by promoting apical localization of integrin β1 and we identify ADP-ribosylation factor 6 (Arf6) as an important effector of ephrin B1 reverse signaling in apical adhesion of APs. Our results provide evidence for an important role for ephrin B1 in maintaining the structural integrity of the developing cortex and highlight the importance of tightly controlling apical cell-ECM adhesion for neuroepithelial development.

KEY WORDS: Ephrin, Cell adhesion, Integrin, Arf6, Exencephaly, Radial glia, Mouse

INTRODUCTION

Apical progenitors (APs) in the developing cortex include neuroepithelial cells, radial glia cells and short neural progenitors (Fietz and Huttner, 2011; Götz and Huttner, 2005). Common features of APs are apicobasal polarity and possession of an apical endfoot lining the ventricular surface. Apical processes provide attachment between neighboring cells via the formation of adherens junctions, which are required for cortical integrity (Kadowaki et al., 2007). Adherens junctions, together with bundles of F-actin running parallel to the apical plasma membrane, form the adherens belt, an important structure that imparts rigidity during epithelial morphogenesis (Yonemura, 2011). In addition to cell-cell adhesion via adherens junctions, apical processes of APs also provide adhesion to the extracellular matrix (ECM) present at the ventricular surface (Loulier et al., 2009).

Complete or partial loss of apical adhesion or polarity is necessary at several steps of development of the neural tube. For instance, local alteration in the apical adhesion and polarity of neuroepithelial cells allows for flexibility of the neuroepithelium and is required for hinge-point formation during neurulation (Eom et al., 2011). Furthermore, loss of apical contact by asymmetric division is associated with a change of fate during the neurogenic period (Götz and Huttner, 2005; Shitamukai et al., 2011). Lastly, increased delamination of neural progenitors from the apical ventricular surface could be responsible for the emergence of a class of basal progenitors (BPs) that may have occurred at the beginning of cortical expansion during evolution (Fietz and Huttner, 2011).

[1]Centre de Biologie du Développement, CNRS, 118 Route de Narbonne, Bât 4R3, 31062 Toulouse cedex 9, France. [2]Université de Toulouse, UPS, F-31062, France. [3]Département Neurotransmission et Sécrétion Neuroendocrine, Institut des Neurosciences Cellulaires et Intégratives, CNRS UPR-3212 and Université de Strasbourg, 5 rue Blaise Pascal, 67084 Strasbourg, France. [4]Department of Cell and Tissue Biology and Program in Craniofacial and Mesenchymal Biology, University of California San Francisco, San Francisco, CA 94143-0442, USA.

*Author for correspondence (alice.davy@univ-tlse3.fr)

Accepted 7 March 2013

The mechanisms by which apical adhesion events are regulated during neural tube development and neurogenesis are under intense scrutiny and a number of studies have identified key molecular effectors that control assembly and/or maintenance of cadherin-based adherens junctions, including cell-fate determinants such as Numb and Numbl, and small GTPases (Chen et al., 2006; Katayama et al., 2011; Rasin et al., 2007). By contrast, how integrin-based adhesion of apical progenitors is regulated is currently unknown.

Eph receptors and ephrins form a large family of cell surface proteins that regulate various aspects of development (Nievergall et al., 2012). A distinctive feature of the Eph/ephrin signaling pathway is the ability of both Eph receptors and ephrins to activate signal transduction cascades (respectively called forward and reverse signaling) and its extensive cross-talk with other cell surface receptors, including cadherins and integrins (Arvanitis and Davy, 2008). Although Eph/ephrin signaling is commonly associated with cell repulsion, a number of studies have shown that this signaling cascade might also promote cell-cell and cell-ECM adhesion in certain cellular contexts (Halloran and Wolman, 2006). We are particularly interested in ephrin B1 as it is encoded by an X-linked gene mutation of which causes the human craniofrontonasal syndrome (CFNS) (Twigg et al., 2004; Wieland et al., 2004). CFNS is an unusual congenital disorder in which heterozygote female patients exhibit a number of defects that are not observed in hemizygote male carriers. We and others have shown that this is due to the formation of ectopic Eph-ephrin boundaries within developing tissues of heterozygote individuals (Compagni et al., 2003; Davy et al., 2006). In the developing cortex, ephrin B1 is expressed in APs from the neuroepithelial stage in a ventricular-high to pial-low gradient (Stuckmann et al., 2001). Ephrin B1 is required to maintain the neural progenitor fate at late stages of cortical development (Murai et al., 2010; Qiu et al., 2008) and we have shown recently that ephrin B1 reverse signaling controls the switch between progenitor maintenance and neuronal differentiation by engaging in a feedback loop involving miR-124, a pro-neuronal miRNA (Arvanitis et al., 2010).

Here, we report that a fraction of *Efnb1*$^{-/-}$ and *Efnb1*$^{+/-}$ embryos display exencephaly, which led us to consider a potential role for ephrin B1 in neuroepithelial morphogenesis. We show that *Efnb1* mutants exhibit neuroepithelial morphological defects that appear before the onset of neurogenesis and persist throughout cortical development. These morphological alterations are characterized by an irregular appearance of the apical surface of the neuroepithelium and formation of micro-invaginations at the apical surface of the ventricular zone (VZ). These morphological alterations are accompanied by a misplacement of mitotic nuclei within the cortical wall without changes in apicobasal polarity of APs. Using *ex vivo* electroporation, we demonstrate that ephrin B1 is required to maintain apical adhesion of APs. Furthermore, we show that ephrin B1 reverse signaling inhibits the ADP-ribosylation factor 6 (Arf6) in APs and controls integrin-based cell-ECM apical adhesion.

MATERIALS AND METHODS

Animals

Wild-type (*Efnb1*$^{+/+}$), *Efnb1*$^{+/-}$ female, *Efnb1*$^{-/-}$ female and *Efnb1*$^{Y/-}$ male mice were generated as described (Davy et al., 2004) and kept in a mixed 129S4/C57BL/6J genetic background. For clarity in embryonic studies, *Efnb1*$^{-/-}$ refers to *Efnb1*-null embryos of both genders. *Efnb1*$^{F6/F6}$ and *Efnb1*$^{DV/DV}$ mice were described previously (Bush and Soriano, 2009). *Efnb1*$^{lox/lox}$ mice were described previously (Davy et al., 2004) and kept in a pure 129S4 genetic background. Animal procedures were pre-approved by the Animal Care Committee of Région Midi-Pyrénées (MP/07/21/04/11).

Brain sample preparation

Timed-pregnant mice were sacrificed by cervical dislocation; embryos were removed and dissected in ice-cold PBS. For immunohistochemistry, embryonic brain tissues were collected and placed in 4% paraformaldehyde (PFA) at 4°C. All brain samples were removed from PFA and either equilibrated in 70% ethanol and embedded in paraffin or immediately sectioned on a vibratome. Coronal paraffin sections (7 μm) were placed on Superfrost microscope slides (Fisher Scientific) and stored at room temperature until use. For quantitative RT-PCR, E13.5 cortices were dissected and total RNAs were extracted with TRI Reagent (Molecular Research Center).

Quantitative RT-PCR (qRT-PCR)

Reverse transcription (RT) was performed with 1 μg of total RNA per reaction. For the qRT-PCR reaction, the resultant cDNA was diluted 1:50. Each RT step was performed in duplicate and the qRT-PCR in triplicate for each RT reaction. RT-PCR was performed using Quantitech SYBR Green Master Mix (Qiagen) and amplified on a Bio-Rad cycler. Relative values were calculated by the $2^{-\Delta\Delta CT}$ method. *U6* RNA was used as an endogenous control. Results are expressed as a percentage of mRNA level compared with the control condition. Experiments were performed in triplicate. Primer sequences were as follows: *S16*F, 5′-AGGAGCGATTTGCTGGTGTGG-3′; *S16*R, 5′-GCTACCAGGGCCTTTGAGATGG-3′; *Efnb1*F, 5′-TTGGCCAAGAACCTGGAG-3′; *Efnb1*R, 5′-GCCCTTCCCACT-TAGG-AACT-3′; *Efnb2*F, 5′-CTGTGCCAGACCAGACCAAGA-3′; *Efnb2*R, 5′-CAGCAGAACTTGCATCTTGTC-3′; *Efnb3*F, 5′-TTCTGC-GAGTGGGACAAAGTC-3′; *Efnb3*R, 5′-GGTCTCTCTCCATGGG-CATTT-3′; *EphB2*F, 5′-gaaggagctcagtgagtacaac-3′; *EphB2*R, 5′-GCACCTGGAAGACATAGATGG-3′; *EphA4*F, 5′-AGTTCCAGAC-CGAACACAGCCT-3′; *EphA4*R, 5′-GCCATGCATCTGCTGCATCTG-3′; *Itgb1*F, 5′-TCTCACCAAAGTAGAAAGCAGG-3′; *Itgb1*R, 5′-ACGATAGCTTCATTGTTGCCAT-3′.

Immunohistochemistry

Paraffin and vibratome sections used for immunohistochemistry were blocked in 5% horse serum in PBS containing 0.1% Triton X-100. Primary antibodies were against ephrin B1 (1:50, R&D Systems), phospho-ephrinB (1:100, Cell Signaling Technology), nestin (1:2, Developmental Studies Hybridoma Bank), N-cadherin (1:2, Developmental Studies Hybridoma Bank), β-catenin (1:1000, Sigma), integrin β1 (1:100, BD Biosciences), P-H3 (1:250, Millipore), GFP (1:100, Millipore), MPM-2 (1:1000, Upstate Biotechnology), Pax6 (1:100, Covance) and Arf6 (1:50, Abcam). Phalloidin-rhodamine was used to label F-actin (DRAQ5, Invitrogen). Images were acquired using a Confocal Leica SP2; single confocal sections are presented except for images of *ex vivo* electroporation, which were acquired on a Confocal Leica SP5. For quantification, the distance between P-H3+ nuclei and the ventricular surface was measured using ImageJ and divided by the width of the cortical wall. P-H3+ nuclei located at the interface with the cortical plate were excluded from the analysis. Alternatively, P-H3+ nuclei were quantified according to their position in the cortical wall. Three bins were defined: apical, corresponding to nuclei touching the ventricular surface; displaced, corresponding to nuclei located at least one nucleus diameter away from the ventricular surface; basal, corresponding to nuclei at the interface between the subventricular zone and the cortical plate. For quantification of cell number, paraffin sections of embryonic day (E) 13.5 embryos were counterstained with DAPI and a 100 μm^2 counting box was placed across three different counting regions in the cortex. Triplicate measurements were performed on six sections per sample, n=3 per genotype.

Cell culture

Cultures of primary neural progenitor cells (NPCs) were performed as described previously (Chojnacki and Weiss, 2008). Briefly, E14.5 cortices (three mice per genotype) were dissected mechanically in Hank's Buffer Saline Solution (HBSS; Invitrogen), followed by enzymatic digestion using a trypsin cocktail (40 mg/ml trypsin, 20 mg/ml Type I-S hyaluronidase, and 4 mg/ml kynurenic acid) in HBSS. The single-cell suspension was collected, rinsed with DMEM/F-12 (Invitrogen) and cultured with growing media [DMEM/F-12 medium containing 0.6% glucose, 5 mM HEPES, 1 mM putrescine, 5 ng/ml basic fibroblast growth factor (FGF2), 20 ng/ml epidermal growth factor (EGF), 10 ng/ml insulin-transferrin-sodium selenite supplement and 2% B27 supplement] in a 5% CO_2 incubator at 37°C. Ephrin B1^{deltaC} corresponds to amino acids 1-268 of mouse ephrin B1. Hek cells were transiently transfected with either pcDNA3.1, ephrin B1^{WT} or ephrin B1^{deltaC}. These cells were incubated with EphB2-Fc, fixed and immunostained with an antibody directed against the cytoplasmic tail of ephrin B1 (C18, Santa Cruz Biotech).

Adhesion assay

Twenty-four-well tissue culture plates were coated overnight at 4°C with solutions containing either PBS, PBS + 4 μg/ml EphB2-Fc, PBS + 4 μg/ml EphA4-Fc or laminin (10 μg/ml). Alternatively, plates were coated with PBS + 1 μg/ml laminin in presence or absence of 4 μg/ml of EphB2-Fc or EphA4-Fc. NPCs were trypsinized, washed, re-suspended in full media and 10×10^4 cells were plated in triplicate in the coated wells. Plates were incubated (37°C, 15 minutes) and unattached cells were removed by aspiration. Attached cells were fixed in 4% PFA for 10 minutes at room temperature, washed and stained with Crystal Violet. After extensive rinsing, Crystal Violet was extracted in 1 ml 2% SDS and optical density of the resulting solution was measured at 550 nm. Alternatively, NPCs were incubated for 5 minutes with a control IgG or a function-blocking antibody to integrin β1 (3.5 μg; BD Pharmingen) prior to the adhesion assay.

Pull down and western blotting analysis

Cortices from E13.5 embryos were lysed in 0.5 ml ice cold lysis buffer (20 mM Tris, pH 8.0), 100 mM NaCl, 1 mM $MgCl_2$, 1% Triton X-100, 0.05% cholate, 0.01% SDS, 1 mM dithiothreitol, 1 mM phenylmethylsulfonyl fluoride, 5 μg/ml aprotinin, 5 μg/ml leupeptin, 1 mM NaF, 1 mM vanadate). Protein lysates were clarified by centrifugation at 14,000 rpm (16,000 ***g***) for 10 minutes at 4°C. For the detection of integrin β1, 25 μg of total lysate was subject to SDS-PAGE. Proteins were transferred onto nitrocellulose membrane, incubated with primary antibodies to integrin β1 (BD Biosciences) and Grb2 (Millipore). For Arf6 activity assays, lysates were immediately incubated with 10 μg of GST-MT2 fusion protein conjugated with glutathione beads, in the presence of 2 mM $ZnCl_2$ for 2 hours at 4°C with rocking, as previously described (Béglé et al., 2009). The beads were collected and washed with PBS containing 2 mM $ZnCl_2$, 1 mM phenylmethylsulfonyl fluoride, 5 μg/ml aprotinin,

5 μg/ml leupeptin, 1 mM NaF and 1 mM vanadate. Bound proteins were dissociated and denatured by heating to 100°C for 10 minutes in 100 μl SDS loading buffer. Aliquots were subject to SDS-PAGE on a 12% gel. Western blots were carried out with anti-ARF6 antibodies. Alternatively, NPCs were dissociated and 10×10^6 cells were incubated for 15 or 60 minutes with 4 μg/ml pre-clustered EphB2-Fc at 37°C. Control samples were incubated with 4 μg/ml pre-clustered IgG-Fc. NPCs were lysed and lysates were processed as described above for Arf6 activity.

Ex vivo electroporations and organotypic slice cultures

E14.5 embryos were decapitated and electroporations were performed as described (Arvanitis et al., 2010). Briefly, solutions containing 5 μg/μl expression vectors were mixed with 0.01% Fast Green and injected into the telencephalon ventricles using pulled 3.5-NanoLTR needles. Five electrical pulses were applied (50 V, 50 mseconds duration, 1-second intervals) using a BTX ECM-830 electroporator (BTX, Gentronic). Electroporated heads were kept in ice-cold PBS with 5% glucose, dissected and embedded in 3% agarose. Vibratome sections (250 μm) corresponding to the dorsolateral region of the cortex were cultured for 20-24 hours in neurobasal medium supplemented with N2 (Invitrogen), B27 (Invitrogen), 0.1% penicillin-streptomycin and 2 mM l-glutamine. Slices were then fixed with 4% PFA and processed for immunostaining with rhodamine phalloidin (1:500) or integrin β1 (1:200; Epitomics). Images were acquired using a BiPhoton Leica SP5. The images were then imported into ImageJ and the distance between GFP+ cells and the ventricular surface was measured (arbitrary units), averaged and then divided by the total distance corresponding to the width of the cortical wall. Measurements (between 50 and 70 per section) were performed on four sections per sample; n=9 GFP, n=10 Cre, n=9 Cre + ephrin B1-GFP, n=9 Cre + ephrin-B1deltaC, n=8 Cre + Arf6T27N, and n=6 Arf6WT, n=6 Arf6Q67L. Quantification of apical processes was performed as described previously (Loulier et al., 2009). Briefly, E14.5 electroporated cortices were stained with phalloidin to label the actin belt at the ventricle surface. 70- to 90-μm z-stacks were collected in 4-μm steps and each z-stack was analyzed with LSM examiner (Zeiss) to determine the fraction of GFP+ cells possessing an apical process attached to the ventricle (as determined by colocalization between GFP and actin). Alternatively, the ratio between the number of soma and the number of apical contacts (as determined by colocalization between GFP and actin) was quantified on confocal z-sections. Counts were averaged from four stacks of n=5 cortices for each condition. For some analysis, electroporated thick sections were cultured for 24 hours and cells were dissociated in a solution of trypsine/DNAse. Dissociated cells were fixed and immunostained in suspension. An aliquot of the cell suspensions was analyzed and quantified under the microscope.

Statistical analysis

Mean, standard deviation and *P*-values were calculated using Excel software. Student's *t*-test was performed to determine significant differences between samples. A value of $P<0.05$ was considered statistically significant.

RESULTS

Neuroepithelial morphological defects in *Efnb1* mutants

A significant fraction of *Efnb1*$^{+/-}$ and a small number of *Efnb1*$^{-/-}$ mutant embryos exhibit exencephaly [*Efnb1*$^{+/+}$: 0/57 embryos; *Efnb1*$^{+/-}$: 11/49 embryos (22.4%); *Efnb1*$^{-/-}$: 9/117 embryos (7.69%); supplementary material Fig. S1], suggesting that ephrin B1 might be required for morphogenesis of the neural tube. Accordingly, ephrin B1 is expressed in nestin-positive neuroepithelial cells at early stages of development, where it is enriched in the apical region (Fig. 1A). To understand how ephrin B1 could influence neuroepithelial morphogenesis, we performed an immunohistochemical analysis of *Efnb1* mutants; however, to circumvent secondary effects that could be caused by neural tube closure defects, we selected only mutant embryos that had undergone neural tube closure. At E10.5, we observed that the gross

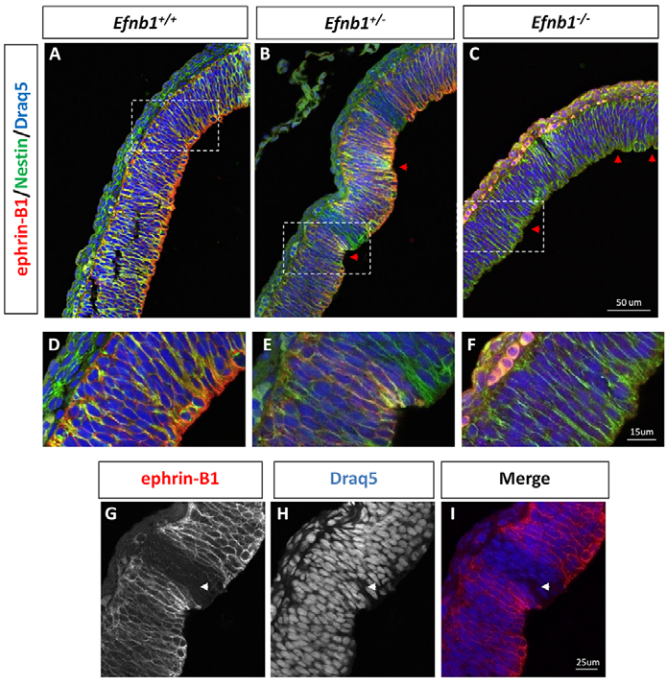

Fig. 1. Ephrin B1 is required for neuroepithelium morphogenesis. (**A-C**) E10.5 sagittal sections from WT (A), *Efnb1*$^{+/-}$ (B) and *Efnb1*$^{-/-}$ (C) embryos were stained for nestin (green) and ephrin B1 (red). Draq5 (blue) was used to label nuclei. Abnormal folding of the neuroepithelium (red arrowheads) could be observed in *Efnb1*$^{+/-}$ and *Efnb1*$^{-/-}$ mutants. (**D-F**) Magnified view of the area outlined in the dashed boxes in A-C showing abnormal folding of the apical surface of the neuroepithelium in *Efnb1* mutants. (**G-I**) E10.5 sagittal sections from an *Efnb1*$^{+/-}$ embryo were stained for ephrin B1 (red); Draq5 (blue) was used to label nuclei. Ephrin B1 staining shows segregation of ephrin B1-positive cells and ephrin B1-negative cells in the neuroepithelium. Abnormal gaps between nuclei are present in ephrin B1-negative domains (arrowhead).

morphology of the forebrain neuroepithelium was normal in *Efnb1* mutants, yet the neuroepithelial apical surface appeared abnormally folded in *Efnb1*$^{+/-}$ (n=3/3) and *Efnb1*$^{-/-}$ (n=2/3) embryos compared with wild-type (WT) embryos (n=3) (Fig. 1A-F; supplementary material Fig. S1). In keeping with a higher penetrance of the exencephaly phenotype in *Efnb1*$^{+/-}$ embryos, we observed a more drastic morphological phenotype in these embryos (Fig. 1B). Owing to random X-inactivation, *Efnb1*$^{+/-}$ embryos are mosaic for ephrin B1 expression and, as has been shown in other tissues (Compagni et al., 2003; Davy et al., 2004; Davy et al., 2006), ephrin B1-positive cells and ephrin B1-negative cells segregate in different territories in the neuroepithelium (Fig. 1G). We noted the appearance of abnormal gaps between nuclei in ephrin B1-negative domains (Fig. 1G-I), suggesting that the integrity of the neuroepithelium was compromised in the absence of ephrin B1.

Because expression of ephrin B1 persists in APs at later stages of cortical development (Stuckmann et al., 2001), we wondered what would be the consequences of *Efnb1* loss of function for development of the neocortex. To study the physiological function of ephrin B1 and to avoid phenotypes that could be due to formation of ectopic Eph-ephrin boundaries in *Efnb1*$^{+/-}$ embryos, we decided to focus our analysis on *Efnb1*$^{-/-}$ embryos. We used acetylated tubulin to visualize the VZ and differentiated neurons in the cortical plate of WT and *Efnb1*$^{-/-}$ forebrain. At this developmental stage, differentiation and migration of newborn neurons seemed

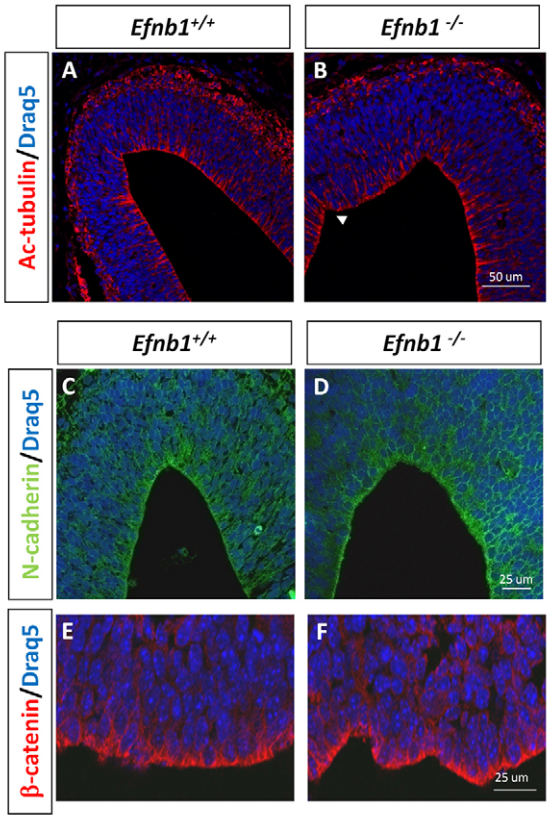

Fig. 2. Morphological defects do not correlate with changes in cell polarity in *Efnb1* mutants. (**A**,**B**) E13.5 coronal sections of WT or *Efnb1*$^{-/-}$ forebrain were stained for acetylated tubulin (red) and Draq5 (blue, nuclei). Ectopic invaginations of the apical surface of the VZ (arrowhead) are detected in *Efnb1*$^{-/-}$ embryos. (**C**,**D**) Coronal sections of E13.5 WT or *Efnb1*$^{-/-}$ forebrain were stained for N-cadherin (green) and Draq5 (blue, nuclei). (**E**,**F**) Coronal sections of E16.5 WT and *Efnb1*$^{-/-}$ embryos were stained with an antibody to β-catenin (red) to assess apicobasal polarity.

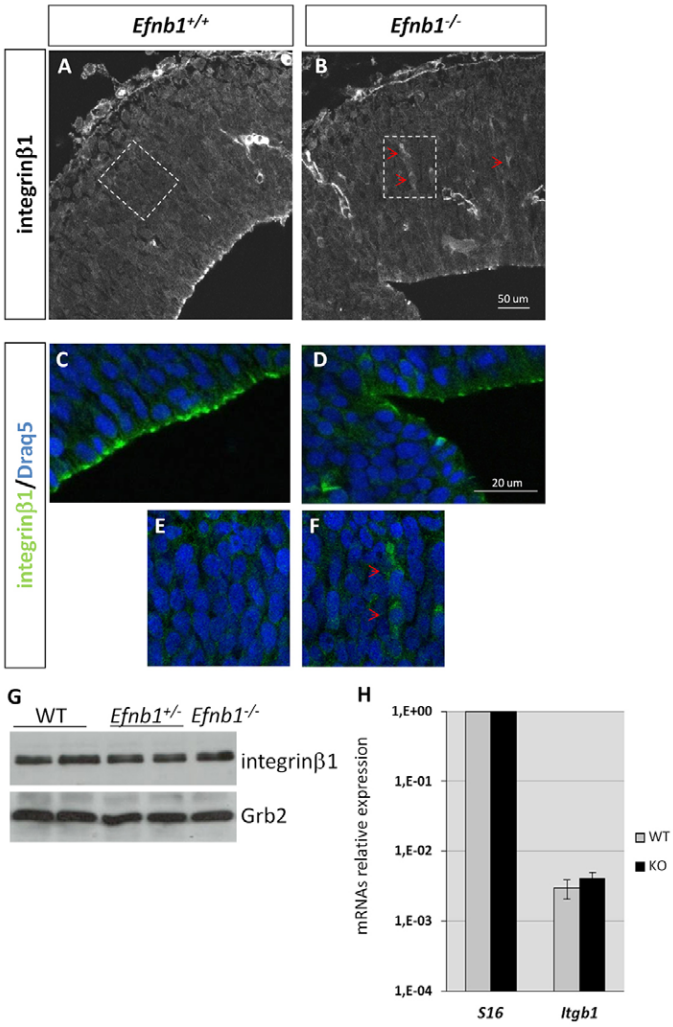

Fig. 3. Ephrin B1 regulates the apical distribution of integrin β1 in APs. (**A-F**) Coronal sections of E13.5 WT (A,C,E) or *Efnb1*$^{-/-}$ (B,D,F) forebrain were stained for integrin β1 and nuclei were labeled with Draq5. (C,D) High-magnification images showing decreased localization of integrin β1 at the apical surface of the VZ in *Efnb1* mutants (D) compared with WT (C). (E,F) High-magnification images corresponding to the boxed areas in A and B showing ectopic cytoplasmic staining in a subset of cells in the VZ of *Efnb1* mutants (F) compared with WT (E). Red arrowheads indicate diffuse intracellular staining. (**G**) Western blotting for integrin β1 from E13.5 WT, *Efnb1*$^{+/-}$ and *Efnb1*$^{-/-}$ cortical homogenates shows no change in the level of integrin β1 in mutant cortices compared with WT. Grb2 was used as a loading control. (**H**) Expression of *Itgb1* in the cortex of E13.5 WT (gray bars) and *Efnb1*$^{-/-}$ (black bars) embryos was analyzed by quantitative RT-PCR. No difference in *Itgb1* mRNA levels was detected in *Efnb1*$^{-/-}$ compared with WT samples.

unaffected by the loss of ephrin B1 (Fig. 2A,B). However, we observed that *Efnb1* mutant embryos exhibited micro-invaginations of the ventricular surface that were not observed in WT embryos (Fig. 2A,B; *Efnb1*$^{+/-}$: 7/9 embryos; *Efnb1*$^{-/-}$: 7/11 embryos). Similar micro-invaginations, visible at high magnification, were also present at E16.5 (*Efnb1*$^{+/-}$: 6/7 embryos; *Efnb1*$^{-/-}$: 3/4 embryos). Altogether, these results indicate that ephrin B1 is required for normal structure of the apical surface of the neuroepithelium.

Epithelial integrity requires local control of apical cell adhesion and polarity, two processes that could be impacted by the loss of ephrin B1. Immunostaining for N-cadherin (cadherin 2) indicated that this protein was normally expressed and localized in *Efnb1* mutants (Fig. 2C,D). To test whether cell polarity was affected by the loss of ephrin B1, we used β-catenin as a marker of apicobasal polarity and observed that apical distribution of β-catenin was also normal in *Efnb1* mutants (Fig. 2E,F). These results indicate that morphological defects observed in *Efnb1* mutants were not correlated with a loss of apicobasal polarity or cadherin-based cell-cell adhesion.

Apical distribution of integrin β1 at the ventricular surface is impaired in *Efnb1* mutants

In addition to cell-cell adhesion, cell-ECM adhesion also takes place at the apical surface of the VZ. Indeed, integrin β1 localizes at the apical surface of the VZ, where it engages laminin to maintain apical adhesion of APs (Loulier et al., 2009). To test whether loss of ephrin B1 impacts integrin-based adhesion, we performed immunostaining for integrin β1 on sections of E13.5 *Efnb1*$^{+/+}$ and *Efnb1*$^{-/-}$ embryos. We observed a marked decrease of integrin β1 apical localization concomitant with the appearance of a diffuse intracellular staining in a subset of cells in the VZ of *Efnb1* mutants (n=4/5) that was not observed in WT (n=0/4) (Fig. 3A-F). This decrease in apical staining was not due to an overall decrease in integrin β1 protein levels (Fig. 3G) or

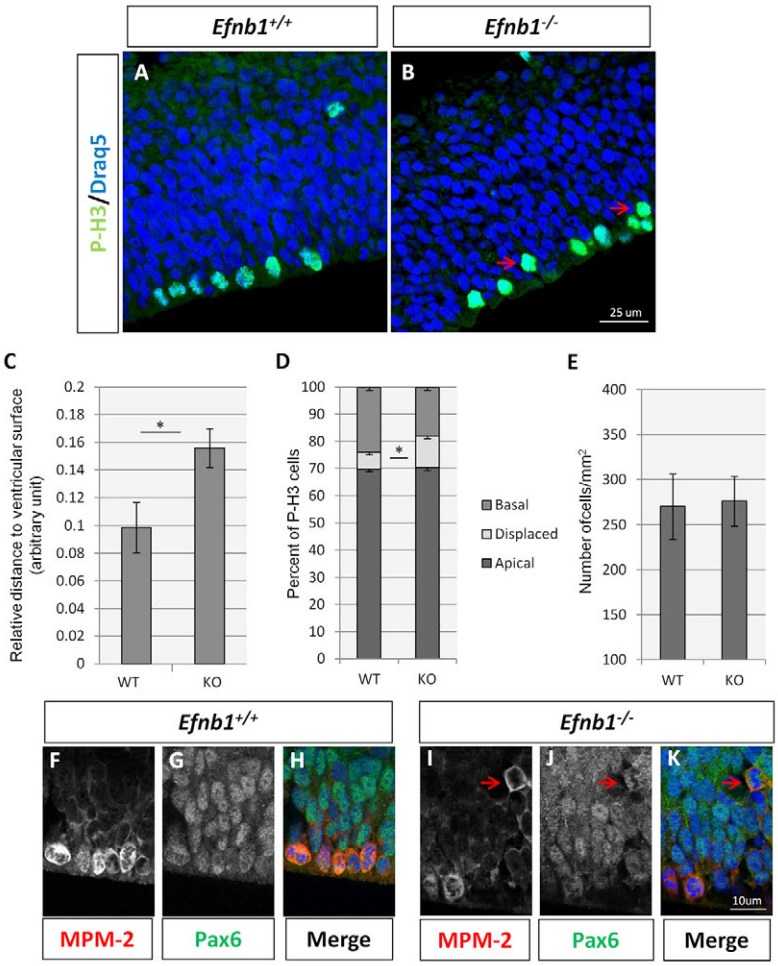

Fig. 4. Displacement of mitotic nuclei in *Efnb1* mutants. (**A**,**B**) Coronal sections of E13.5 WT (A) and *Efnb1*$^{-/-}$ (B) forebrain were stained for P-H3 and nuclei were labeled with Draq5. Note the displacement of mitotic nuclei in *Efnb1*$^{-/-}$ embryos (arrows, B). (**C**) Quantification of the distance between P-H3-positive nuclei and the ventricular surface relative to cortical width. (**D**) Quantification of mitotic nuclei according to their position in the VZ (apical: nuclei lining the ventricle; displaced: nuclei at least one nuclei diameter away from the ventricle; basal: nuclei adjacent to the cortical plate). Quantifications were performed on at least 500 P-H3-positive cells from five embryos per genotype. (**E**) Total number of cells in E13.5 WT (n=3) and *Efnb1*$^{-/-}$ (n=3) embryos determined by nuclear counting. For C-E, statistical analysis was performed using Student's t-test. *P<0.05. Error bars represent s.d. (**F-K**) Coronal sections of E13.5 WT (F-H) and *Efnb1*$^{-/-}$ (I-K) embryos were stained for MPM-2 (F,I, red) and Pax6 (G,J, green); nuclei were labeled with Draq5 (blue in H,K). The majority of displaced mitotic nuclei in *Efnb1* mutants (arrows) express Pax6.

mRNA levels (Fig. 3H), indicating that subcellular localization of integrin β1, but not expression, is modified in *Efnb1*-deficient APs.

One of the phenotypes observed following transient abrogation of integrin signaling at the ventricular surface was an increase in the number of mitotic nuclei positioned away from the ventricular surface (Loulier et al., 2009). Because we observed a decrease in integrin β1 apical localization in *Efnb1* mutants, we decided to test whether loss of ephrin B1 also affects the position of mitotic nuclei. Mitotic nuclei were labeled with phospho-histone H3 (P-H3) and the distribution of these nuclei was analyzed in E13.5 WT and *Efnb1*$^{-/-}$ VZ (Fig. 4A,B; supplementary material Fig. S2). Measurement of the distance between P-H3-positive nuclei and the ventricular surface showed that P-H3-positive mitotic nuclei were positioned further away from the apical surface in *Efnb1*$^{-/-}$ VZ compared with WT (Fig. 4A-C). We next quantified the number of P-H3-positive nuclei according to their position in the cortical wall. Although the number of mitotic nuclei at the apical surface was unchanged, the appearance of displaced P-H3-positive nuclei correlated with a decrease in the number of mitotic nuclei corresponding to BPs (adjacent to the cortical plate) in *Efnb1*$^{-/-}$ embryos (Fig. 4D). No change in the total number of cells in the VZ could be detected at this stage (Fig. 4E). Importantly, 62.5% (n=24 nuclei from three *Efnb1*$^{-/-}$ embryos) of displaced mitotic nuclei (labeled with the mitotic marker MPM-2) expressed Pax6, a marker of APs (Fig. 4F-K). The fact that a fraction of displaced nuclei were Pax6 negative suggested that displaced nuclei represent both AP and BP nuclei. We confirmed that a fraction of displaced mitotic nuclei were BPs by performing Tbr2 (Eomes – Mouse Genome Informatics) immunostaining on WT and *Efnb1*$^{-/-}$ mutant cortex (supplementary material Fig. S3). Altogether, these results demonstrate that loss of ephrin B1 impairs the distribution of mitotic nuclei in the cortical wall, a phenotype that is reminiscent of that observed following transient abrogation of integrin β1 signaling at the ventricular surface.

Acute loss of ephrin B1 leads to dispersion of APs

These results prompted us to test the short-term consequences of a loss of ephrin B1 in APs. Acute loss of ephrin B1 was obtained by electroporating an expression vector for Cre recombinase into the developing cortex of *Efnb1*$^{flox/flox}$ embryos and cultivating organotypic slices of electroporated brains. Twenty hours after electroporation, cells electroporated with a control vector and GFP exhibited a typical distribution in the cortical wall with the majority of electroporated cells located in the VZ (Fig. 5A,D,E). By contrast, cells co-electroporated with GFP and Cre recombinase exhibited a dispersed distribution in the cortex, with a significant fraction of these cells displaced away from the VZ (Fig. 5B,D,E). To ensure that these phenotypes were due to the loss of ephrin B1, and not to a non-specific consequence of Cre recombinase expression, we co-electroporated plasmids encoding Cre recombinase and ephrin B1-GFP. Overexpression of ephrin B1-GFP prevented dispersion of Cre-expressing cells away from the VZ (Fig. 5C,D,E). At the cellular level, the majority of control-

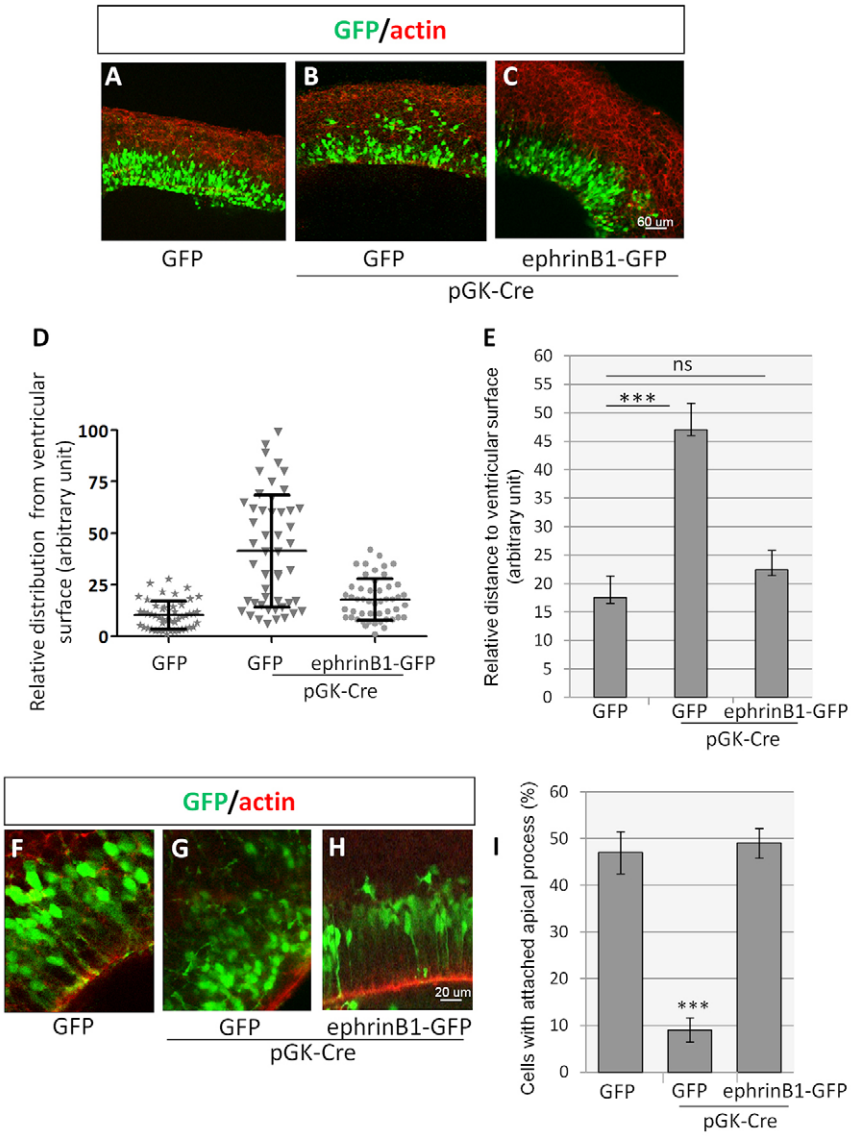

Fig. 5. Acute loss of ephrin B1 leads to detachment of APs from the ventricular surface. (**A-C**) *Ex vivo* electroporation of the developing cortex of *Efnb1*$^{flox/flox}$ E14.5 embryos with GFP (A), pGK-CRE+GFP (B) or pGK-CRE+ephrinB1-GFP (C). Position of electroporated cells was assessed by indirect immunofluorescence detecting GFP on slice cultures (green). The overall organization of the cortex was visualized by staining for F-actin (red). (**D**) Dot plot of the distance between GFP+ cells and the ventricular surface relative to cortical width. Each dot corresponds to measurements for one electroporated cell from one representative brain for each electroporation condition. (**E**) The mean distance between GFP+ cells and the ventricular surface relative to cortical width in the three electroporation conditions (GFP, *n*=9; pGK-CRE+GFP, *n*=10; pGK-CRE+ephrinB1-GFP, *n*=10). (**F-H**) High-magnification images of *Efnb1*$^{flox/flox}$ E14.5 cortices electroporated with GFP (F), pGK-CRE+GFP (G) and pGK-CRE+ephrinB1-GFP (H). Low-magnification (A-C) and high-magnification (F-H) images are from independent electroporated cortices. Images are representative of a minimum of three independent electroporated brains. (**I**) Quantification of the percentage of electroporated cells possessing an apical process contacting the ventricular surface (*n*=5 per condition). Statistical analysis was performed using Student's *t*-test. ***P<0.001; ns, non-significant. Error bars represent s.d.

electroporated cells exhibited an elongated morphology with their apical processes attached to the ventricular surface (Fig. 5F,I; supplementary material Fig. S4). This elongated morphology and contact to the ventricular surface was lost in Cre-electroporated cells located in the VZ (Fig. 5G,I; supplementary material Fig. S4). Co-expression of Cre recombinase and ephrin B1-GFP restored normal elongated morphology of APs and attachment to the ventricular surface (Fig. 5H,I; supplementary material Fig. S4). Importantly, these modifications in cell distribution and morphology were not due to apoptosis (supplementary material Fig. S5). Furthermore, electroporation of Cre recombinase did not change the proportion of GFP-positive cells expressing either Pax6, Tbr2 or β3 tubulin, a marker of neurons (supplementary material Fig. S5), indicating that dispersion of APs in Cre-electroporated slices does not correlate with a change of fate in this short time window. Altogether, these results suggest that ephrin B1 is required to maintain AP adhesion at the apical surface of the ventricle.

Although Eph/ephrin signaling is better known for its role in promoting cell repulsion, interaction between Eph receptors and ephrins can result in increased integrin-mediated adhesion of ephrin-expressing cells in certain cellular contexts (Davy and Robbins, 2000; Huai and Drescher, 2001). To test whether Eph/ephrin B1 signaling directly promoted adhesion of APs, we isolated primary NPCs, which express ephrin B1 (supplementary material Fig. S6), and performed adhesion assays on substrates coated with Eph receptors. We chose EphA4 and EphB2, two of the ephrin B1 cognate receptors that are expressed in the developing E13.5 neocortex in a pattern overlapping with that of ephrin B1 (supplementary material Fig. S7). Quantitative RT-PCR experiments showed that *EphA4* is more highly expressed than *EphB2* in the developing neocortex (supplementary material Fig. S7), yet EphB2 is the preferred interacting receptor for ephrin B1 (supplementary material Fig. S8) (Noberini et al., 2012). First, we tested the ability of NPCs to directly bind to EphB2-, EphA4- or laminin-coated culture plates. NPCs exhibited a slight, but not significant, decrease in adhesion to plates coated with EphB2-Fc or EphA4-Fc, compared with plates coated with PBS or laminin (Fig. 6A). Next, we tested whether Eph-ephrin B1 interaction could modulate integrin-mediated adhesion. Culture plates were coated with a solution containing either laminin, laminin + EphB2-Fc, or laminin + EphA4-Fc, and adhesion of NPCs to these substrates was evaluated. NPCs exhibited a preferential adhesion to plates coated with laminin + EphB2-Fc compared with plates coated with laminin

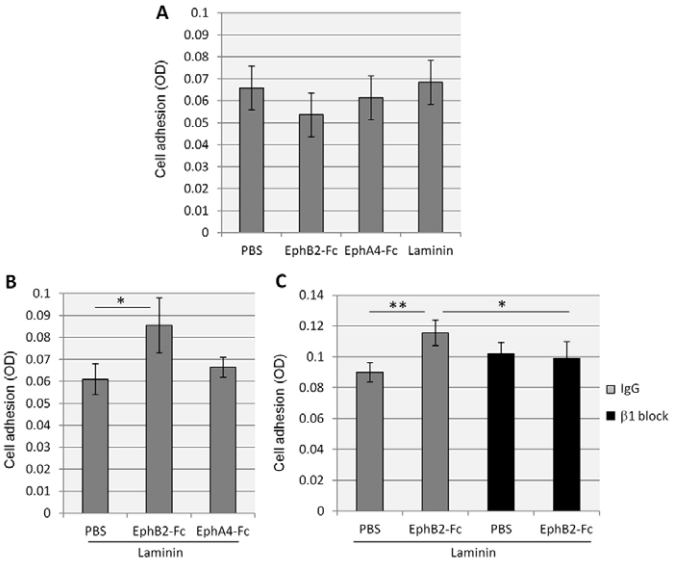

Fig. 6. EphB2-ephrin B1 interaction promotes integrin β1-mediated adhesion in neural progenitors. (**A**) Adhesion of WT NPCs to plates coated with PBS, EphB2-Fc, EphA4-Fc or laminin. (**B**) Adhesion of WT NPCs to plates coated with PBS + laminin, EphB2-Fc + laminin, or EphA4-Fc + laminin. Data are from four independent experiments. (**C**) Adhesion of WT NPCs to plates coated with PBS + laminin or EphB2-Fc + laminin in the absence or presence of an integrin β1-blocking antibody. Data are from three independent experiments. Statistical analysis was performed using Student's *t*-test. **P*<0.05, ***P*<0.01. Error bars represent s.d. OD, optical density.

alone or laminin + EphA4-Fc (Fig. 6B). Importantly, increased adhesion of NPCs on laminin + EphB2-Fc was blocked in presence of an integrin β1 function-blocking antibody (Fig. 6C), indicating that EphB2-ephrin B1 interaction promoted integrin-mediated adhesion of NPCs.

Altogether, these results suggest that ephrin B1, via an interaction with EphB2 on neighboring cells, maintains morphology and distribution of APs in the VZ by promoting apical integrin-based adhesion.

SH2- and PDZ-dependent reverse signaling is dispensable for apical adhesion of APs

To characterize the molecular mechanisms by which ephrin B1 controls integrin-based adhesion of APs, we tested the requirement of the ephrin B1 signaling domains for cortical morphogenesis. Two signaling modules have been identified in the cytoplasmic tail of ephrin B1: tyrosines that are phosphorylated in response to activation of the pathway and a binding domain for PDZ-containing proteins. Tyrosine phosphorylation of ephrinBs could be detected in the VZ and in the cortical plate of WT embryos (Fig. 7A) where it colocalized with ephrin B1 in the VZ (Fig. 7A-C). Because ephrin B1 is the most highly expressed ephrinB in the neo-cortex and in NPCs (supplementary material Figs S6, S7), these results strongly suggest that ephrin B1 is tyrosine phosphorylated in APs.

To test whether tyrosine phosphorylation or binding to PDZ-containing proteins are required for VZ morphogenesis, we analyzed embryos expressing mutant versions of ephrin B1 that are lacking these signaling modules either individually or in combination (Bush and Soriano, 2009). No structural abnormality was detected in the cortex of these mutant embryos and integrin β1 was properly localized at the apical surface of the VZ (Fig. 7D-F). Furthermore, exencephaly has never been observed in these mutants (J. O. Bush, personal communication). These results indicate that both of these signaling modules are dispensable for structuration of the neuroepithelium.

To evaluate directly the requirement of the ephrin B1 cytoplasmic domain for apical adhesion of APs, we generated a truncated version of ephrin B1 in which the entire cytoplasmic domain was deleted (ephrin-B1^{deltaC}). We confirmed *in vitro* that this truncated form of ephrin B1 was expressed at the cell surface and was able to interact with EphB2 (supplementary material Fig. S8A-C). Surprisingly, co-electroporation of Cre recombinase and ephrin-B1^{deltaC} in the developing cortex of *Efnb1*$^{flox/flox}$ embryos was sufficient to restore the distribution of APs in the VZ (Fig. 7G-I), indicating that the cytoplasmic domain of ephrin B1 is not required for apical adhesion of APs. Interestingly, expression of ephrin-B1^{deltaC} was sufficient to induce adhesion and spreading of HeLa cells on a substrate containing EphB2-Fc (supplementary material Fig. S9D-H), suggesting that this truncated form of ephrin B1 retains some signaling activity.

Ephrin B1 regulates adhesion of APs via inhibition of Arf6

The small GTPase Arf6 has been shown to influence cell-ECM interactions by regulating recycling of integrins in migratory cells (Pellinen and Ivaska, 2006). Furthermore, Arf6 has recently been identified as an effector of EphA2-mediated adhesion in cultured epithelial cells (Miura et al., 2009). This prompted us to test whether this cytosolic protein could play a role downstream of ephrin B1 in APs. Immunohistochemistry for Arf6 revealed that this GTPase is expressed in APs, where it is enriched at the apical surface similar to ephrin B1 (Fig. 8A,B). We next set out to investigate whether Arf6 activity was modified in *Efnb1* mutants. Metallothionein 2 has been shown to interact specifically with Arf6-GTP, the active form of Arf6 (Schweitzer and D'Souza-Schorey, 2002); we thus performed pull-down assays using a GST- metallothionein 2 fusion protein to specifically pull down active Arf6-GTP from E13.5 cortical protein lysates. These experiments revealed that Arf6 activity was dramatically increased in the cortex of *Efnb1*$^{-/-}$ (Fig. 8C), suggesting that ephrin B1 normally restrains Arf6 activity. To test this hypothesis directly, we stimulated cultured NPCs with EphB2-Fc and monitored Arf6 activity using GST-metallothionein 2 pull down. EphB2-Fc stimulation for 15 minutes led to a decrease in the level of Arf6-GTP (Fig. 8D,E), indicating that ephrin reverse signaling directly inhibits Arf6 activity in NPCs. We next evaluated the consequences of increased Arf6 activity on APs, by expressing a constitutively active form of Arf6 (Arf6^{Q67L}) in these cells. Constitutive activation of Arf6 led to cell dispersion and the appearance of cells that did not attach to the ventricular surface (Fig. 9A-F). In addition, the constitutively activated form of Arf6 blocked adhesion and spreading of HeLa cells in response to ephrin B1 reverse signaling (supplementary material Fig. S10). Conversely, co-expression of a dominant-negative form of Arf6 (Arf6^{T27N}) was able to rescue the dispersion phenotype induced by acute loss of ephrin B1 (Fig. 9G-J). These results suggest that inhibition of Arf6 activity downstream of ephrin B1 reverse signaling is necessary to maintain apical adhesion of APs.

DISCUSSION

Ephrin B1 and cortical development

Ephrin B1 controls a number of processes in the developing cortex, including maintenance of progenitor fate, guidance of callosal axons

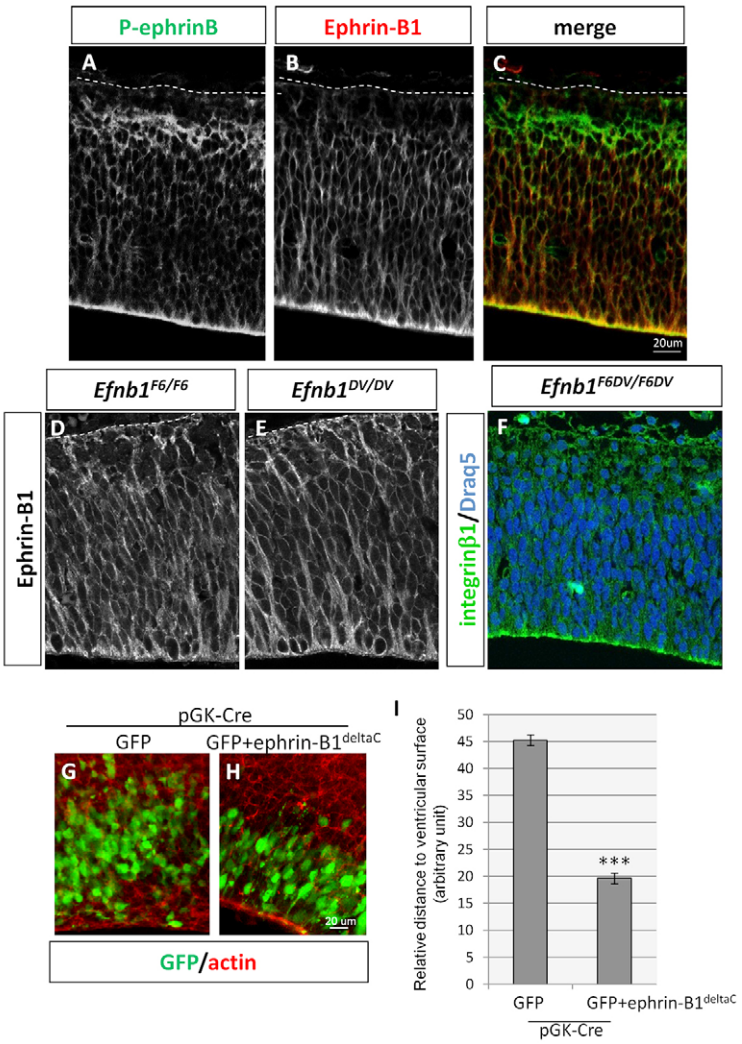

Fig. 7. The cytoplasmic domain of ephrin B1 is dispensable for apical adhesion of APs. (**A-C**) Coronal sections of a WT E13.5 embryo were stained with an antibody specific to tyrosine phosphorylated ephrinBs (P-ephrinB; A, green) and with an antibody specific to ephrin B1 (B, red). (**D-F**) Coronal sections from *Efnb1* mutant embryos in which tyrosine phosphorylation is prevented (*Efnb1*^{F6}; D) or mutants in which binding to PDZ-domain-containing proteins is prevented (*Efnb1*^{DV}; E) were stained for ephrin B1. (F) Coronal sections of E13.5 *Efnb1*^{F6DV} embryos were stained for integrin β1 (green) and nuclei were labeled with Draq5 (blue). Dashed lines highlight the pial surface of the cortex. (**G-I**) *Efnb1*$^{flox/flox}$ E14.5 embryos were co-electroporated with either pGK-CRE + GFP + empty vector (G) or with pGK-CRE + GFP + ephrin-B1^{deltaC} (H). Distribution of electroporated cells was assessed by indirect immunofluorescence detecting GFP on slice cultures (green). The overall organization of the cortex was visualized by staining for F-actin (red). (I) Quantification of the mean distance between GFP+ cells and the ventricular surface relative to cortical width (pGK-CRE + GFP + empty vector, n=10; pGK-CRE + GFP + ephrin-B1^{deltaC}, n=9). Statistical analysis was performed using Student's t-test. ***P<0.001. Error bars represent s.d.

and migration of projection neurons in a reelin-dependent manner (Arvanitis et al., 2010; Bush and Soriano, 2009; Qiu et al., 2008; Sentürk et al., 2011). Here, we demonstrate that ephrin B1 is also implicated in neural tube morphogenesis by promoting adhesion of APs to the ventricular surface. Importantly, our data show that ephrin B1 exerts this function as early as the neuroepithelial stage, before its implication in neurogenesis, which has been shown to take place at later stages of development (Qiu et al., 2008). Specifically, a decrease in the number of P-H3-positive cells was observed in the VZ of *Efnb1* mutants at E16.5 but not at E13.5 (Qiu

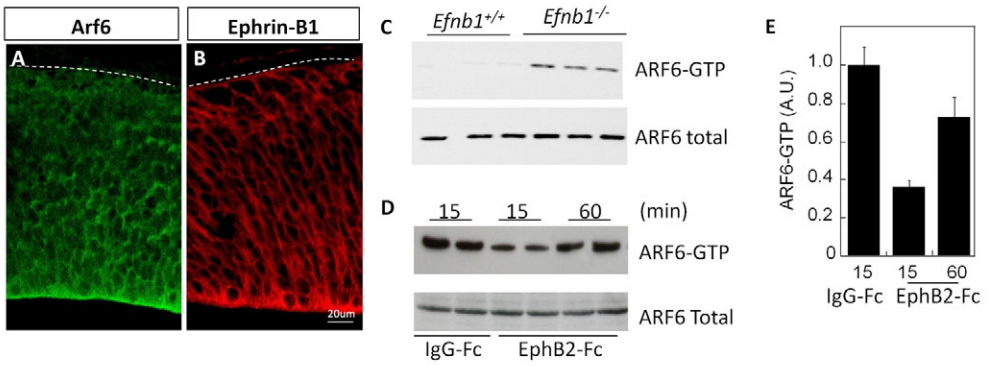

Fig. 8. Ephrin B1 reverse signaling inhibits Arf6 activity. (**A**,**B**) Coronal sections of E13.5 embryos were stained for Arf6 (A, green) and for ephrin B1 (B, red). Dashed lines highlight the pial surface of the cortex. (**C**) Arf6 activity is increased in the cortex of *Efnb1* mutants (*Efnb1*$^{-/-}$) compared with wild-type (WT) E13.5 embryos. Active Arf6 (Arf6-GTP) was pulled down from protein lysates obtained from the cortex of three independent embryos of each genotype using metallothionein 2 (Mt2)-GST beads. Total Arf6 levels in the lysates are shown. (**D**,**E**) Cultured NPCs were stimulated with IgG-Fc or with EphB2-Fc and Arf6 activity was monitored using GST-metallothionein 2 pull-down. Total Arf6 levels in the lysates are shown. (E) Quantification of Arf6-GTP compared with total Arf6 protein is shown for IgG-Fc and EphB2-Fc stimulation. Error bars represent s.d.

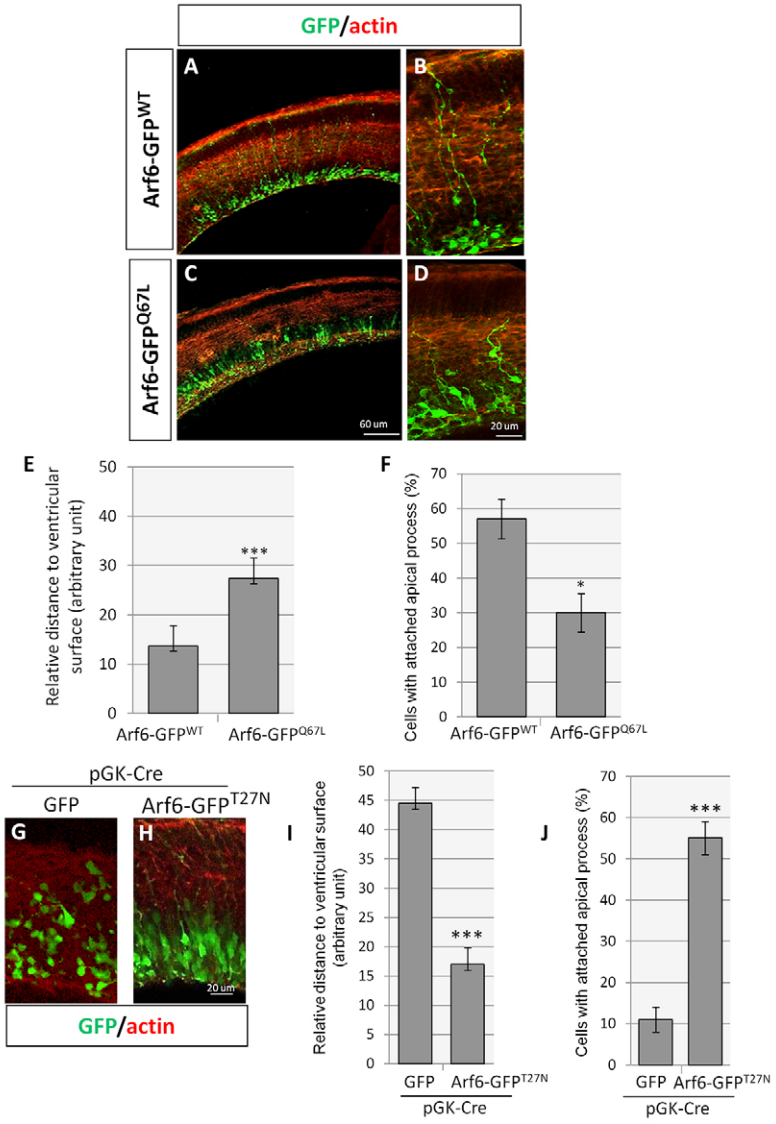

Fig. 9. Ephrin B1 reverse signaling regulates adhesion of APs via Arf6. (**A-D**) Wild-type Arf6-GFP^{WT} (A,B) and constitutively active Arf6-GFP^{Q67L} (C,D) were electroporated in wild-type E14.5 cortex and morphology of APs was assessed by indirect immunofluorescence detecting GFP on *ex vivo* slice cultures (green). The overall organization of the cortex was visualized by staining for actin (red). (**E**) Quantification of the mean distance between GFP+ cells and the ventricular surface relative to cortical width (n=6 electroporated brains per condition). (**F**) Quantification of the percentage of electroporated cells possessing an apical process contacting the ventricular surface (n=3 per condition). (**G**,**H**) *Ex vivo* electroporation of the developing cortex of *Efnb1*$^{flox/flox}$ E14.5 embryos with pGK-CRE + GFP (G) and pGK-CRE + Arf6-GFP^{N27T} (H). Cell distribution was assessed by indirect immunofluorescence detecting GFP on *ex vivo* slice cultures (green). The overall organization of the cortex was visualized by staining for actin (red). (**I**) Quantification of the mean distance between GFP+ cells and the ventricular surface relative to cortical width (pGK-CRE + GFP, n=9; pGK-CRE + Arf6-GFP^{N27T}, n=8). (**J**) Quantification of the percentage of electroporated cells possessing an apical process contacting the ventricular surface (n=5 per condition). Images are representative of a minimum of three independent electroporated brains. Statistical analysis was performed using Student's t-test. *P<0.05, ***P<0.001. Error bars represent s.d.

et al., 2008) (data not shown). Although the PDZ domain of ephrin B1 is required for its role in neurogenesis (Qiu et al., 2008), we showed here that it is dispensable for adhesion of APs, supporting the notion that both functions are distinct.

Despite a well-known role for Eph/ephrin signaling in promoting cell repulsion, our data show that in APs, ephrin B1 promotes integrin-based cell adhesion. EphA4 and EphB2 are expressed in the developing cortex, where EphA4/ephrin B1 signaling has been implicated in neurogenesis (North et al., 2009). We propose here that EphB2-ephrin B1 interaction may preferentially control adhesion of APs to the apical surface of the VZ. Promotion of cell adhesion has been described previously for the EphA7-ephrin A5 pair and, interestingly, neural tube closure defects (NTDs) are observed in a fraction of *EfnA5*$^{-/-}$ embryos (Holmberg et al., 2000). However, the mechanisms causing NTDs in *EfnA5*$^{-/-}$ and *Efnb1*$^{-/-}$ are different. In the former study, it was shown that EphA7 and ephrin A5 are expressed at the edge of the dorsal neural folds and that lack of interaction between these proteins led to a failure of the neural folds to fuse at the midline (Holmberg et al., 2000). Here, we show that ephrin B1 plays a structural role at the apical surface of the neuroepithelium. In absence of ephrin B1, local alterations of the apical surface might weaken the rigidity and cohesion of the neuroepithelium and thus perturb the complex morphogenetic processes taking place during neurulation. Our exencephaly data indicate that *Efnb1*$^{+/-}$ are more severely affected than *Efnb1*$^{-/-}$ embryos, which has been reported for other phenotypes observed in mice and humans carrying mutations in *Efnb1* (Compagni et al., 2003; Davy et al., 2004; Twigg et al., 2004; Wieland et al., 2004). Our interpretation for neuroepithelial morphogenesis is that in *Efnb1*$^{+/-}$ embryos, sorting between ephrin B1-positive and ephrin B1-negative cells leads to discontinuous rigidity of the neuroepithelium, which is more detrimental to morphogenesis of this tissue than a homogenous decrease in rigidity. One of the phenotypes we observed that could be linked to a decrease in rigidity of the cortical tissue in *Efnb1*$^{-/-}$ mutants is the mis-positioning of mitotic nuclei of both APs and BPs. Indeed, it has long been proposed that apical-to-basal migration of nuclei could be a passive mechanism driven by cell crowding (Sauer, 1935). More recently, it has been shown that weakening the apical acto-myosin cortex in APs leads to defects in apical-to-basal nuclear migration of both APs and BPs (Schenk et al., 2009). Lastly, blocking integrin β1 function at the apical surface of the cortex leads to mis-positioning of mitotic nuclei (Loulier et al., 2009).

Mechanisms of ephrin-induced adhesion

We showed that ephrin B1 controls apical adhesion of APs by an indirect mechanism involving integrin β1. Indeed, in cultured NPCs, Eph-ephrin interaction promoted cell adhesion only in presence of laminin. Furthermore, acute loss of ephrin B1 led to the dispersion of APs in the cortical wall, a phenotype reminiscent of that observed when apical integrin β1 is specifically targeted using function-blocking antibodies or in laminin α2-deficient embryos (Loulier et al., 2009). Lastly, we observed that the distribution of integrin β1 at the apical membrane of APs was perturbed in *Efnb1*$^{-/-}$ embryos. A number of studies have reported regulation of integrin-based adhesion by Eph/ephrin signaling (Arvanitis and Davy, 2008; Davy and Robbins, 2000; Huai and Drescher, 2001). Although most of these studies were based on *in vitro* data, a crosstalk between Eph/ephrin and integrins has previously been demonstrated *in vivo* during somitogenesis in the zebrafish embryo (Jülich et al., 2009). Interestingly, the latter study showed that ephrin reverse signaling was sufficient to induce clustering of integrin along tissue boundaries.

Our results with ephrin-B1^{deltaC} showed that the extracellular domain of ephrin B1 was able to rescue cell adhesion independently of the cytoplasmic domain. One possible explanation for these results is that this truncated form of ephrin B1 might retain signaling activity, similar to glycosylphosphatidylinositol (GPI)-linked ephrins. Indeed, we have shown previously that activation of reverse signaling via the GPI-linked ephrin A5 led to increased cell-ECM adhesion that was mediated by the inside-out activation of integrin β1 (Davy and Robbins, 2000). Regardless of how ephrin-B1^{deltaC} modulates cell adhesion, our results call for caution in interpreting *in vivo* data using truncated versions of ephrins, which are widely used to discriminate between forward or reverse signaling (Davy and Soriano, 2005).

Arf6 and cell adhesion

We identified Arf6 as an effector of ephrin B1-induced adhesion of APs. We showed that Arf6 activity was increased in *Efnb1* mutant cortex and demonstrated that EphB2/ephrinB1 signaling suppresses Arf6 activity in NPCs. Whether this inhibition involves the engagement or recruitment of the ArfGAP Git1 as was shown previously for EphA2 (Miura et al., 2009) will have to be explored further but is likely to involve a mechanism not described thus far.

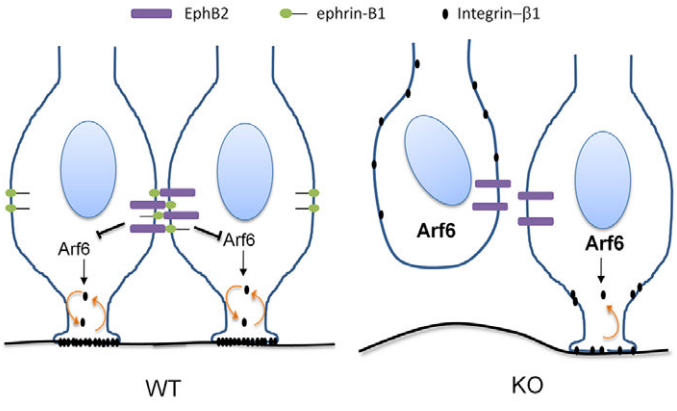

Fig. 10. Model depicting ephrin B1-mediated events in APs. In wild-type APs (WT), Eph/ephrin signaling inhibits Arf6 activity, maintains apical localization of integrin β1 and promotes attachment of APs to the ventricular surface. In the absence of ephrin B1 (KO), levels of active Arf6-GTP rise and integrin β1 is no longer maintained at the apical membrane, thus leading to cell detachment.

Indeed, engagement of Git1 by ephrinB reverse signaling has been reported previously; however, this recruitment required binding of Git1 to Grb4 (Nck2 – Mouse Genome Informatics), which is known to interact with phosphorylated residues on the cytoplasmic tail of ephrinBs (Segura et al., 2007). Here, our findings indicate that engagement of Git1, or any other negative regulator of Arf6, in response to EphB2-ephrin B1 interaction would be achieved independently of the cytoplasmic domain of ephrin B1.

Arf6 is a small GTPase involved in membrane trafficking, plasma membrane protrusions and invaginations, peripheral actin assembly and Ca^{2+}-dependent exocytosis in a number of cell types (D'Souza-Schorey and Chavrier, 2006). Owing to its important bearing on plasma membrane remodeling, Arf6 activity influences morphology, adhesion and migration of numerous cell types. For instance, in epithelial cells, increased Arf6 activity correlated with scattering and the acquisition of a migratory phenotype (Palacios and D'Souza-Schorey, 2003). Arf6 is known to play various roles in neurons, including recycling of integrin β1 to the neuronal surface (Eva et al., 2012), yet a possible function for this small GTPase in the developing cortex has not been reported to date. Our results demonstrate that limiting Arf6 activity is essential for maintaining apical adhesion of APs and ensuring cortical integrity. Our results suggest that low Arf6 activity is required to maintain apical localization of integrin β1 in APs (Fig. 10).

In conclusion, we uncovered an important function for ephrin B1 in maintaining the apical adhesion of APs during cortical development, a function that is essential for appropriate morphogenesis of the neural tube.

Acknowledgements

The Nestin and N-cadherin antibodies were obtained from the Developmental Studies Hybridoma Bank developed under the auspices of the NICHD and maintained by the University of Iowa, Iowa City, IA 52242, USA. We are grateful to Brice Ronsin for his help with confocal microscopy (TRI Imaging Core Facility). We thank the ABC facility and ANEXPLO for housing mice. We thank our laboratory colleagues for critical reading of the manuscript.

Funding

This work was supported by a Career Development Award from the Human Frontier Science Program Organization (HFSPO) [to A.D.]; an ATIP grant from the Centre National de la Recherche Scientifique (CNRS) and a Fondation ARC grant [to A.D.]; and an Agence Nationale de la Recherche (ANR) grant [ANR-09-BLAN-0264-01 to N.V.]. D.N.A. received support from the Fondation pour la Recherche Médicale.

Competing interests statement

The authors declare no competing financial interests.

Supplementary material

Supplementary material available online at
http://dev.biologists.org/lookup/suppl/doi:10.1242/dev.088203/-/DC1

References

Arvanitis, D. and Davy, A. (2008). Eph/ephrin signaling: networks. *Genes Dev.* **22**, 416-429.
Arvanitis, D. N., Jungas, T., Behar, A. and Davy, A. (2010). Ephrin-B1 reverse signaling controls a post-transcriptional feedback mechanism in neural progenitors. *Mol. Cell. Biol.* **30**, 2508-2517.
Béglé, A., Tryoen-Tóth, P., de Barry, J., Bader, M. F. and Vitale, N. (2009). ARF6 regulates the synthesis of fusogenic lipids for calcium-regulated exocytosis in neuroendocrine cells. *J. Biol. Chem.* **284**, 4836-4845.
Bush, J. O. and Soriano, P. (2009). Ephrin-B1 regulates axon guidance by reverse signaling through a PDZ-dependent mechanism. *Genes Dev.* **23**, 1586-1599.
Chen, L., Liao, G., Yang, L., Campbell, K., Nakafuku, M., Kuan, C. Y. and Zheng, Y. (2006). Cdc42 deficiency causes Sonic hedgehog-independent holoprosencephaly. *Proc. Natl. Acad. Sci. USA* **103**, 16520-16525.
Chojnacki, A. and Weiss, S. (2008). Production of neurons, astrocytes and oligodendrocytes from mammalian CNS stem cells. *Nat. Protoc.* **3**, 935-940.
Compagni, A., Logan, M., Klein, R. and Adams, R. H. (2003). Control of skeletal patterning by ephrinB1-EphB interactions. *Dev. Cell* **5**, 217-230.

D'Souza-Schorey, C. and Chavrier, P. (2006). ARF proteins: roles in membrane traffic and beyond. *Nat. Rev. Mol. Cell Biol.* **7**, 347-358.
Davy, A. and Robbins, S. M. (2000). Ephrin-A5 modulates cell adhesion and morphology in an integrin-dependent manner. *EMBO J.* **19**, 5396-5405.
Davy, A. and Soriano, P. (2005). Ephrin signaling in vivo: look both ways. *Dev. Dyn.* **232**, 1-10.
Davy, A., Aubin, J. and Soriano, P. (2004). Ephrin-B1 forward and reverse signaling are required during mouse development. *Genes Dev.* **18**, 572-583.
Davy, A., Bush, J. O. and Soriano, P. (2006). Inhibition of gap junction communication at ectopic Eph/ephrin boundaries underlies craniofrontonasal syndrome. *PLoS Biol.* **4**, e315.
Eom, D. S., Amarnath, S., Fogel, J. L. and Agarwala, S. (2011). Bone morphogenetic proteins regulate neural tube closure by interacting with the apicobasal polarity pathway. *Development* **138**, 3179-3188.
Eva, R., Crisp, S., Marland, J. R., Norman, J. C., Kanamarlapudi, V., ffrench-Constant, C. and Fawcett, J. W. (2012). ARF6 directs axon transport and traffic of integrins and regulates axon growth in adult DRG neurons. *J. Neurosci.* **32**, 10352-10364.
Fietz, S. A. and Huttner, W. B. (2011). Cortical progenitor expansion, self-renewal and neurogenesis-a polarized perspective. *Curr. Opin. Neurobiol.* **21**, 23-35.
Götz, M. and Huttner, W. B. (2005). The cell biology of neurogenesis. *Nat. Rev. Mol. Cell Biol.* **6**, 777-788.
Halloran, M. C. and Wolman, M. A. (2006). Repulsion or adhesion: receptors make the call. *Curr. Opin. Cell Biol.* **18**, 533-540.
Holmberg, J., Clarke, D. L. and Frisén, J. (2000). Regulation of repulsion versus adhesion by different splice forms of an Eph receptor. *Nature* **408**, 203-206.
Huai, J. and Drescher, U. (2001). An ephrin-A-dependent signaling pathway controls integrin function and is linked to the tyrosine phosphorylation of a 120-kDa protein. *J. Biol. Chem.* **276**, 6689-6694.
Jülich, D., Mould, A. P., Koper, E. and Holley, S. A. (2009). Control of extracellular matrix assembly along tissue boundaries via Integrin and Eph/Ephrin signaling. *Development* **136**, 2913-2921.
Kadowaki, M., Nakamura, S., Machon, O., Krauss, S., Radice, G. L. and Takeichi, M. (2007). N-cadherin mediates cortical organization in the mouse brain. *Dev. Biol.* **304**, 22-33.
Katayama, K., Melendez, J., Baumann, J. M., Leslie, J. R., Chauhan, B. K., Nemkul, N., Lang, R. A., Kuan, C. Y., Zheng, Y. and Yoshida, Y. (2011). Loss of RhoA in neural progenitor cells causes the disruption of adherens junctions and hyperproliferation. *Proc. Natl. Acad. Sci. USA* **108**, 7607-7612.
Loulier, K., Lathia, J. D., Marthiens, V., Relucio, J., Mughal, M. R., Tang, S. C., Coksaygan, T., Hall, P. E., Chigurupati, S., Patton, B. et al. (2009). beta1 integrin maintains integrity of the embryonic neocortical stem cell niche. *PLoS Biol.* **7**, e1000176.
Miura, K., Nam, J. M., Kojima, C., Mochizuki, N. and Sabe, H. (2009). EphA2 engages Git1 to suppress Arf6 activity modulating epithelial cell-cell contacts. *Mol. Biol. Cell* **20**, 1949-1959.
Murai, K., Qiu, R., Zhang, H., Wang, J., Wu, C., Neubig, R. R. and Lu, Q. (2010). Gα subunit coordinates with ephrin-B to balance self-renewal and differentiation in neural progenitor cells. *Stem Cells* **28**, 1581-1589.
Nievergall, E., Lackmann, M. and Janes, P. W. (2012). Eph-dependent cell-cell adhesion and segregation in development and cancer. *Cell. Mol. Life Sci.* **69**, 1813-1842.
Noberini, R., Rubio de la Torre, E. and Pasquale, E. B. (2012). Profiling Eph receptor expression in cells and tissues: a targeted mass spectrometry approach. *Cell Adh. Migr.* **6**, 102-112.
North, H. A., Zhao, X., Kolk, S. M., Clifford, M. A., Ziskind, D. M. and Donoghue, M. J. (2009). Promotion of proliferation in the developing cerebral cortex by EphA4 forward signaling. *Development* **136**, 2467-2476.
Palacios, F. and D'Souza-Schorey, C. (2003). Modulation of Rac1 and ARF6 activation during epithelial cell scattering. *J. Biol. Chem.* **278**, 17395-17400.
Pellinen, T. and Ivaska, J. (2006). Integrin traffic. *J. Cell Sci.* **119**, 3723-3731.
Qiu, R., Wang, X., Davy, A., Wu, C., Murai, K. H. Z., Zhang, H., Flanagan, J. G., Soriano, P. and Lu, Q. (2008). Regulation of neural progenitor cell state by ephrin-B. *J. Cell Biol.* **181**, 973-983.
Rasin, M. R., Gazula, V. R., Breunig, J. J., Kwan, K. Y., Johnson, M. B., Liu-Chen, S., Li, H. S., Jan, L. Y., Jan, Y. N., Rakic, P. et al. (2007). Numb and Numbl are required for maintenance of cadherin-based adhesion and polarity of neural progenitors. *Nat. Neurosci.* **10**, 819-827.
Sauer, F. C. (1935). Mitosis in the neural tube. *J. Comp. Neurol.* **62**, 377-405.
Schenk, J., Wilsch-Bräuninger, M., Calegari, F. and Huttner, W. B. (2009). Myosin II is required for interkinetic nuclear migration of neural progenitors. *Proc. Natl. Acad. Sci. USA* **106**, 16487-16492.
Schweitzer, J. K. and D'Souza-Schorey, C. (2002). Localization and activation of the ARF6 GTPase during cleavage furrow ingression and cytokinesis. *J. Biol. Chem.* **277**, 27210-27216.
Segura, I., Essmann, C. L., Weinges, S. and Acker-Palmer, A. (2007). Grb4 and GIT1 transduce ephrinB reverse signals modulating spine morphogenesis and synapse formation. *Nat. Neurosci.* **10**, 301-310.
Sentürk, A., Pfennig, S., Weiss, A., Burk, K. and Acker-Palmer, A. (2011). Ephrin Bs are essential components of the Reelin pathway to regulate neuronal migration. *Nature* **472**, 356-360.
Shitamukai, A., Konno, D. and Matsuzaki, F. (2011). Oblique radial glial divisions in the developing mouse neocortex induce self-renewing progenitors outside the germinal zone that resemble primate outer subventricular zone progenitors. *J. Neurosci.* **31**, 3683-3695.
Stuckmann, I., Weigmann, A., Shevchenko, A., Mann, M. and Huttner, W. B. (2001). Ephrin B1 is expressed on neuroepithelial cells in correlation with neocortical neurogenesis. *J. Neurosci.* **21**, 2726-2737.
Twigg, S. R. F., Kan, R., Babbs, C., Bochukova, E. G., Robertson, S. P., Wall, S. A., Morriss-Kay, G. M. and Wilkie, A. O. M. (2004). Mutations of ephrin-B1 (EFNB1), a marker of tissue boundary formation, cause craniofrontonasal syndrome. *Proc. Natl. Acad. Sci. USA* **101**, 8652-8657.
Wieland, I., Jakubiczka, S., Muschke, P., Cohen, M., Thiele, H., Gerlach, K. L., Adams, R. H. and Wieacker, P. (2004). Mutations of the ephrin-B1 gene cause craniofrontonasal syndrome. *Am. J. Hum. Genet.* **74**, 1209-1215.
Yonemura, S. (2011). Cadherin-actin interactions at adherens junctions. *Curr. Opin. Cell Biol.* **23**, 515-522.

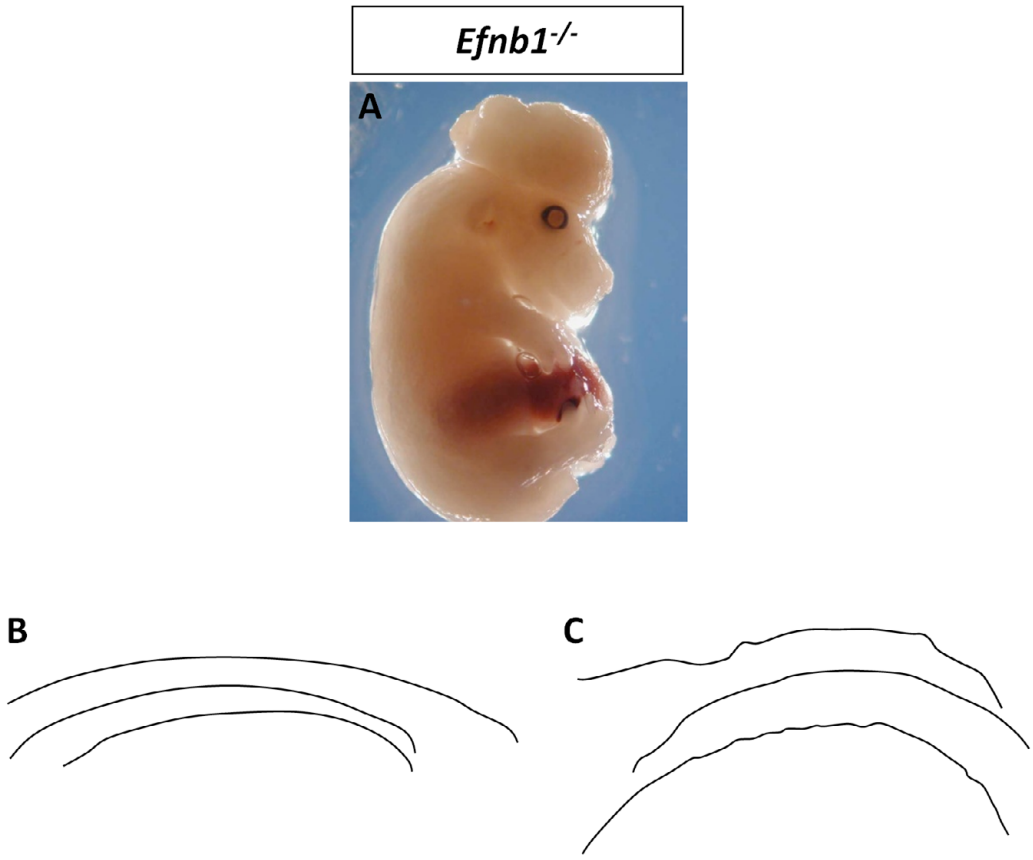

Fig. S1. Exoencephaly in *Efnb1* mutants. (**A**) In addition to omphalocele, this E14.5 *Efnb1* mutant exhibits exencephaly. (**B**,**C**) Camera lucida drawings of the apical surface of the neuroepithelium of three WT (B) and three *Efnb1*$^{-/-}$ (C) embryos. Note the irregular apical surface in *Efnb1* mutants (2/3).

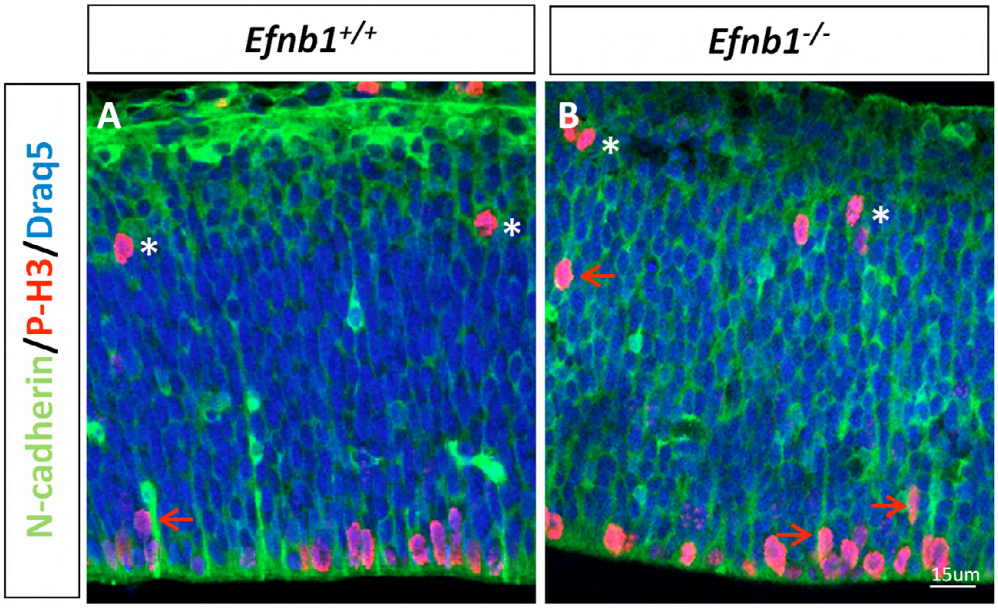

Fig. S2. Altered distribution of mitotic nuclei in the cortical wall of *Efnb1* mutants. (**A**,**B**) Coronal vibratome sections of E13.5 WT (A) and *Efnb1*$^{-/-}$ (B) embryos were stained for N-cadherin (green), P-H3 (red) and Draq5 (blue). Arrows indicate mitotic nuclei positioned away from the ventricular surface. Asterisks indicate basal progenitor nuclei.

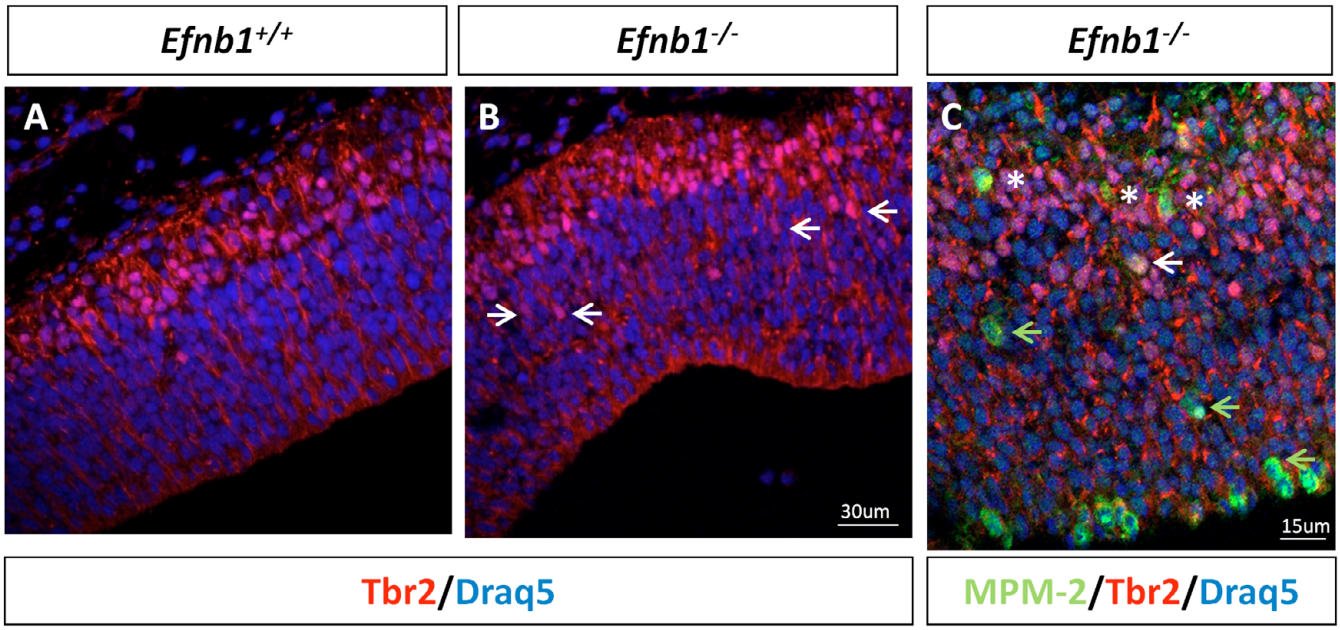

Fig. S3. Altered distribution of mitotic and basal progenitor nuclei in the cortical wall of *Efnb1* mutants. (**A**,**B**) Coronal paraffin sections of WT (A) and *Efnb1*$^{-/-}$ (B) embryos were stained for Tbr2 (red) and Draq5 (blue). Tbr2-positive nuclei are scattered in the cortical wall of *Efnb1*$^{-/-}$ mutants (arrows) (*n*=2/3 embryos). (**C**) Coronal paraffin sections of *Efnb1*$^{-/-}$ embryos were stained for Tbr2 (red), MPM-2 (green) and Draq5 (blue). Asterisks indicate Tbr2-positive basal mitotic nuclei. Arrows indicate mis-positioned mitotic nuclei that are Tbr2 positive (white arrow) or Tbr2 negative (green arrows).

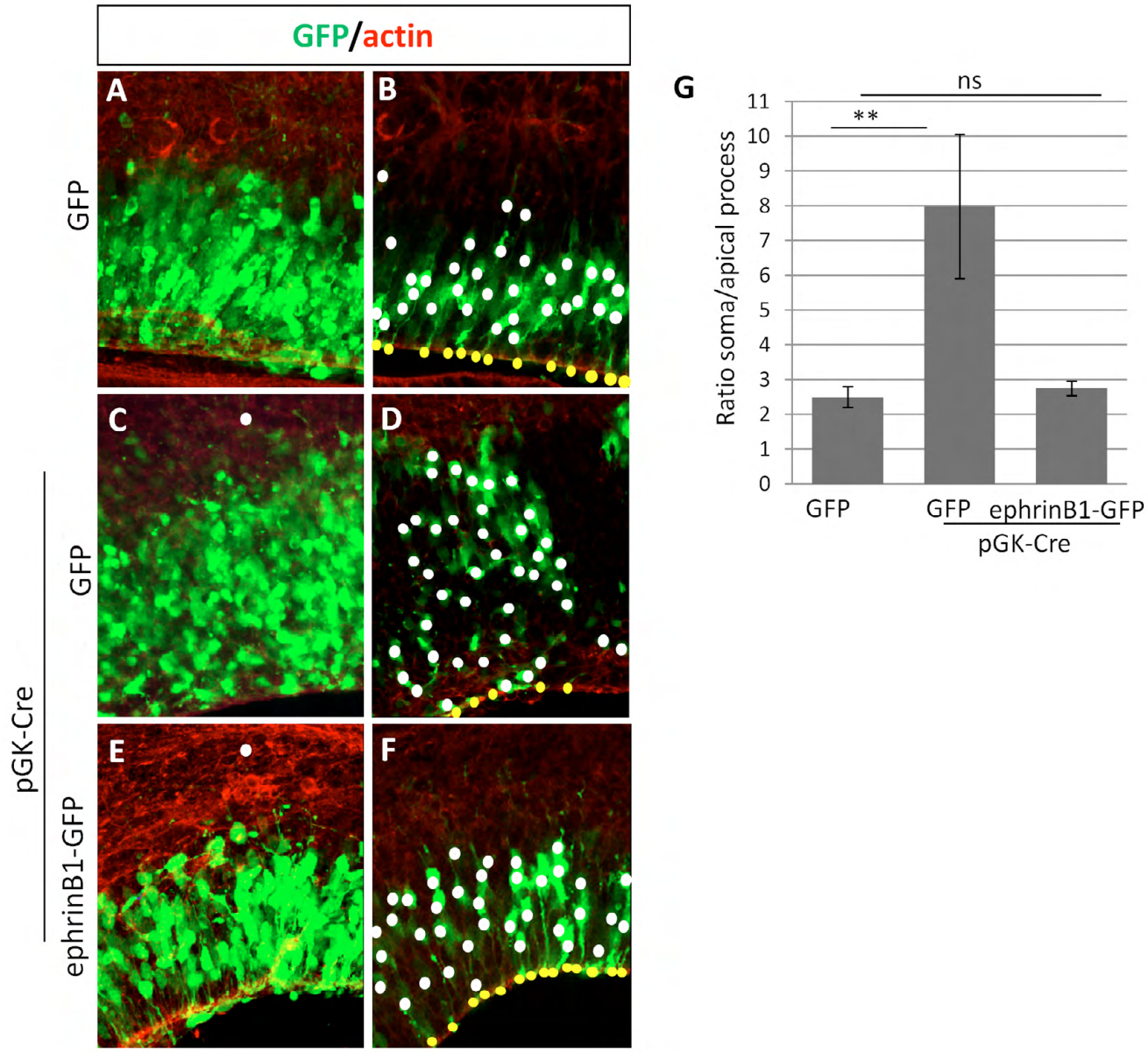

Fig. S4. Targeted excision of *Efnb1* results in apical detachment of neural progenitors (**A-F**) *Ex vivo* electroporation of the developing cortex of *Efnb1*$^{flox/flox}$ E14.5 embryos with GFP (A,B) pGK-CRE+GFP (C,D) and pGK-CRE+ephrinB1-GFP (E,F). The overall organization of the cortex was visualized by staining for F-actin (red). (A,C,E) *z*-stacked images of GFP, pGK-CRE+GFP and pGK-CRE+ephrinB1-GFP electroporated cortices, respectively. (B,D,F) Single *z*-sections of A,C,E, respectively. White dots represent soma, yellow dots represent apical contacts. (**G**) Quantification of the ratio of soma/apical processes in electroporated brains. Images are representative for n=5 for each experimental conditions. Statistical analysis was performed using Student's *t*-test. ns, non-significant; **P<0.01. Error bars represent s.d.

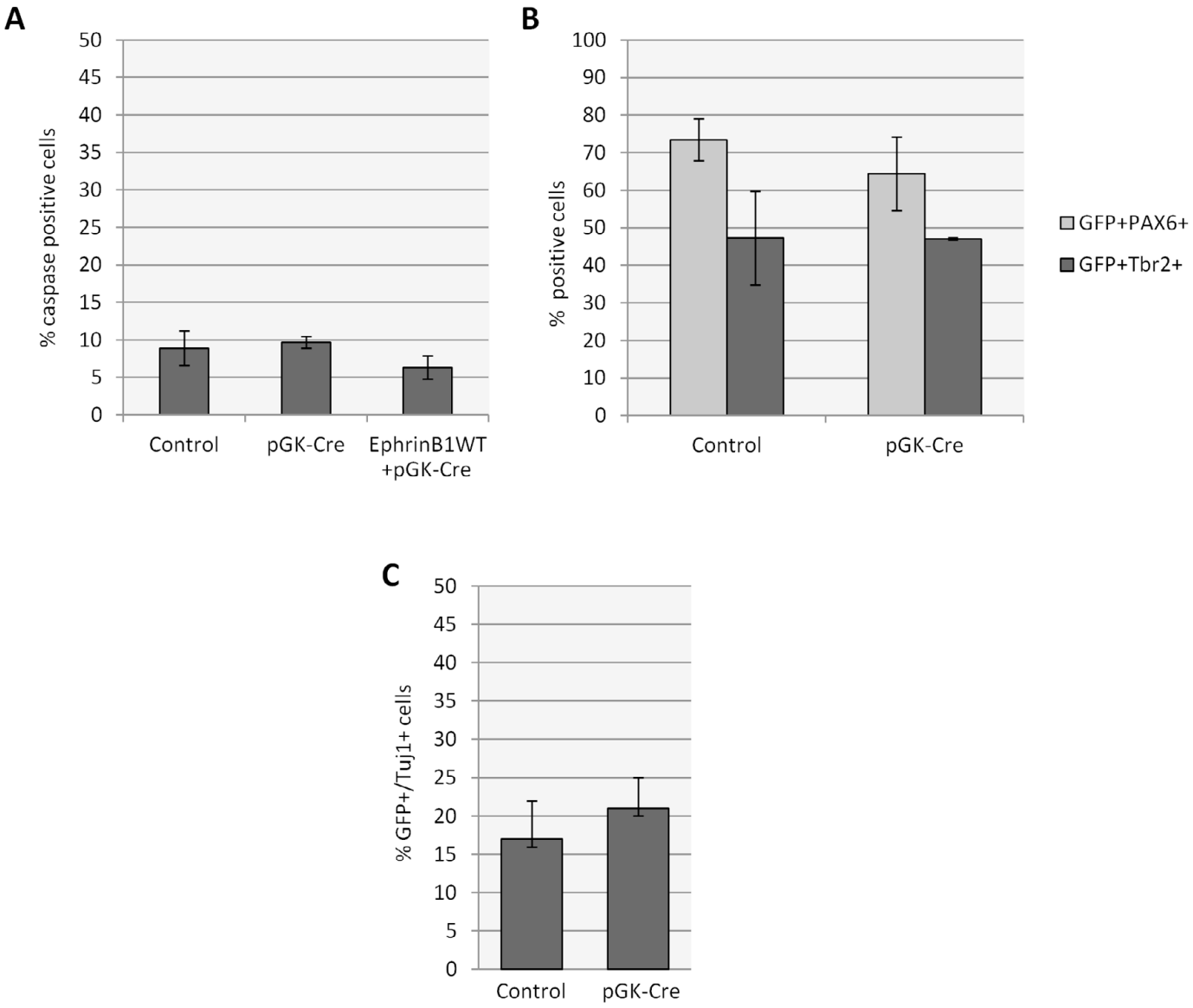

Fig. S5. Characterization of *ex vivo* electroporations. (**A**) E14.5 brains were co-electroporated with GFP and control plasmid or plasmids coding for Cre recombinase or for ephrinB1-GFP. Thick sections were cultured for 24 hours and stained for cleaved caspase. The graph represents the percentage of dissociated GFP-positive cells that were positive for cleaved caspase. At least 300 cells were counted in three independent experiments. Statistical analysis was performed using Student's *t*-test. None of the values was statistically different. (**B**,**C**) E14.5 brain were co-electroporated with GFP and a control plasmid or a plasmid coding for the Cre recombinase. The graphs represent the percentage of dissociated GFP-positive cells that were positive for the markers indicated. At least 150 cells were counted in five independent experiments. Statistical analysis was performed using Student's *t*-test. None of the values was statistically different. Error bars represent s.d.

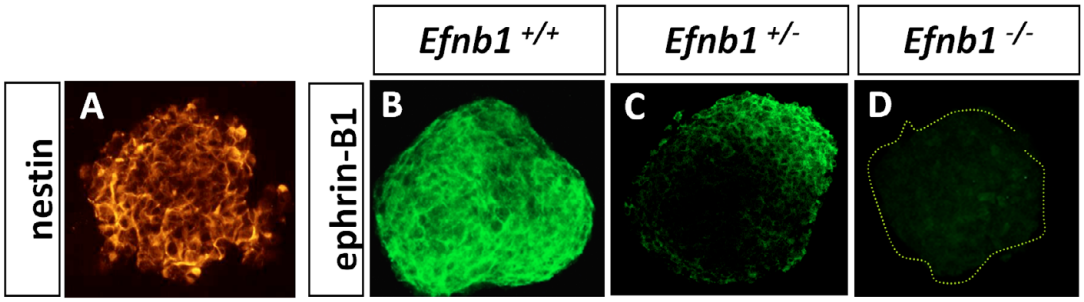

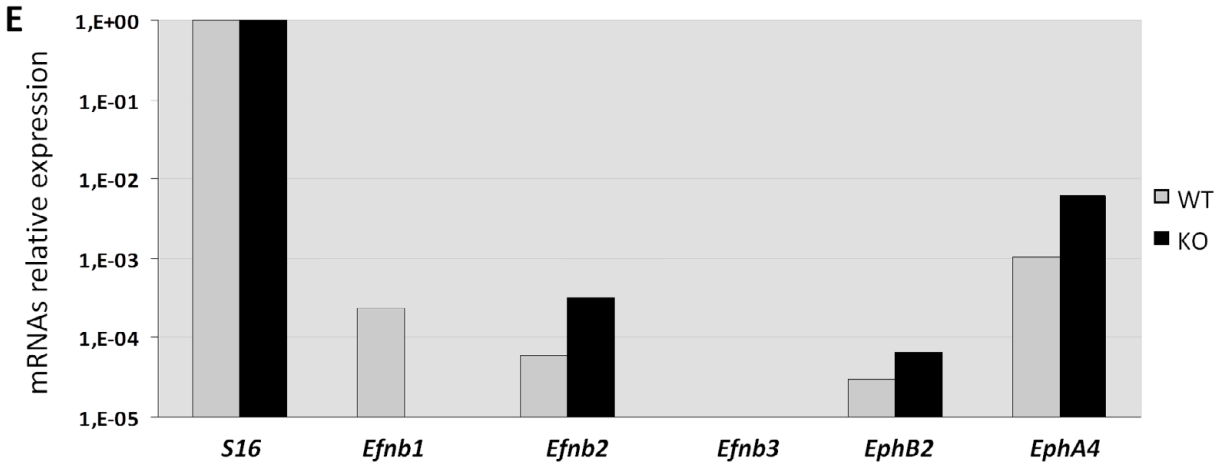

Fig. S6. Characterization of primary neural progenitor cells. (**A**) Neural progenitors (NPCs) grown as neurospheres express nestin. (**B-D**) NPCs were isolated from embryos of different genotypes and expression of ephrin B1 was detected by immunostaining. Sorting between ephrin B1-positive and -negative cells can be visualized in neurospheres isolated from *Efnb1*$^{+/-}$ embryos (C). (**E**) Quantification by qRT-PCR of *S16*, *Efnb1*, *Efnb2*, *Efnb3*, *EphB2* and *EphA4* in NPCs isolated from *Efnb1*$^{+/+}$ (gray bars) and *Efnb1*$^{-/-}$ (black bars) embryos. These results are representative of three independent cultures.

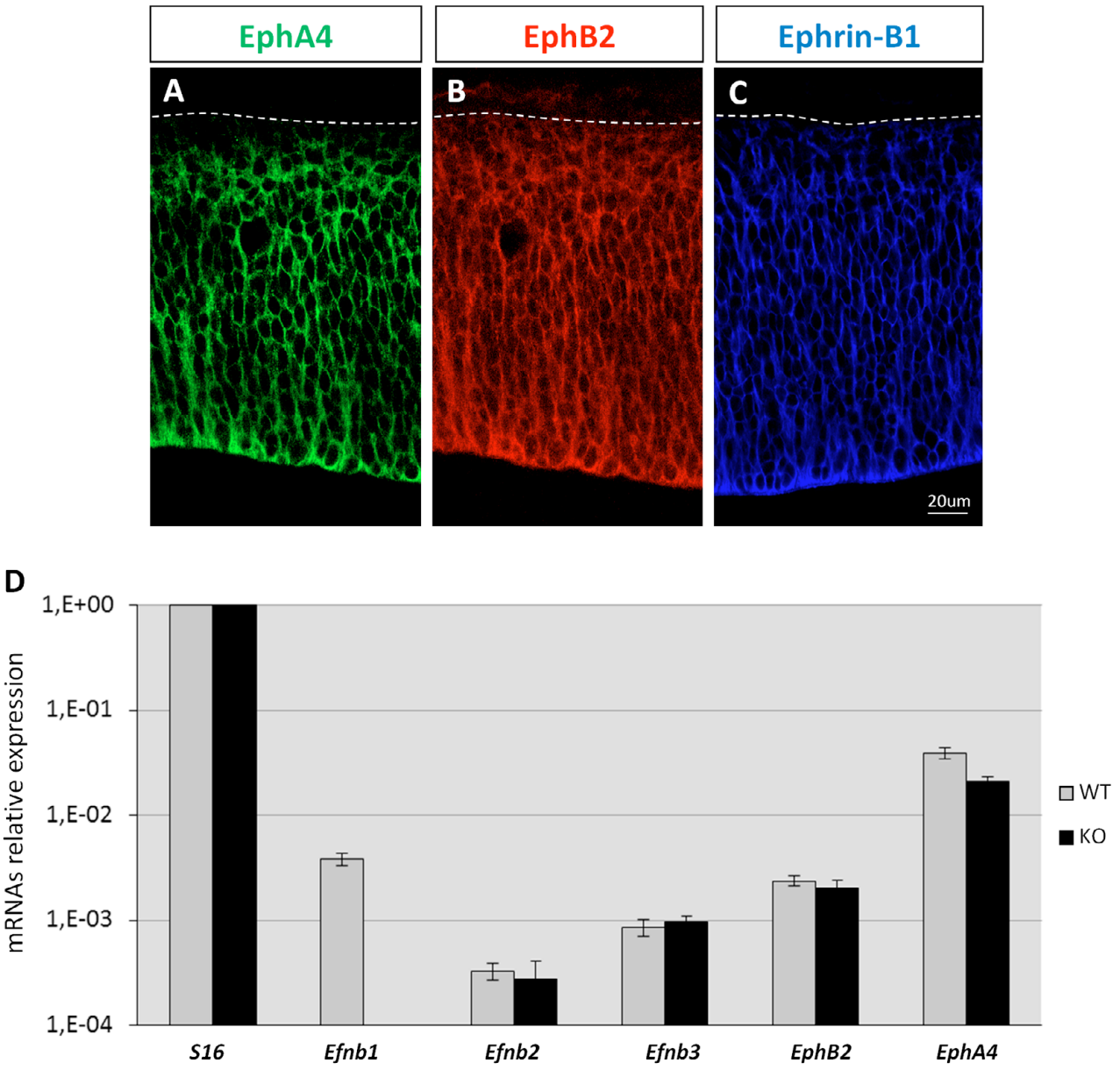

Fig. S7. Expression of Eph and ephrin family members in the developing cortex. (**A-C**) Coronal vibratome sections of E13.5 WT embryos were stained for EphA4 (A, green), EphB2 (B, red) and ephrin B1 (C, blue). Dashed line highlights the pial surface of the cortex. (**D**) Expression of *Efnb1*, *Efnb2*, *Efnb3*, *EphB2* and *EphA4* in the cortex of E13.5 WT (gray bars) and *Efnb1*$^{-/-}$ (black bars) embryos was analyzed by quantitative RT-PCR. *Efnb1* is the most abundant of ephrinBs in the cortex at E13.5. Loss of *EfnB1* does not lead to changes in expression of *Efnb2*, *Efnb3*, *EphB2* or *EphA4.* Error bars represent s.d.

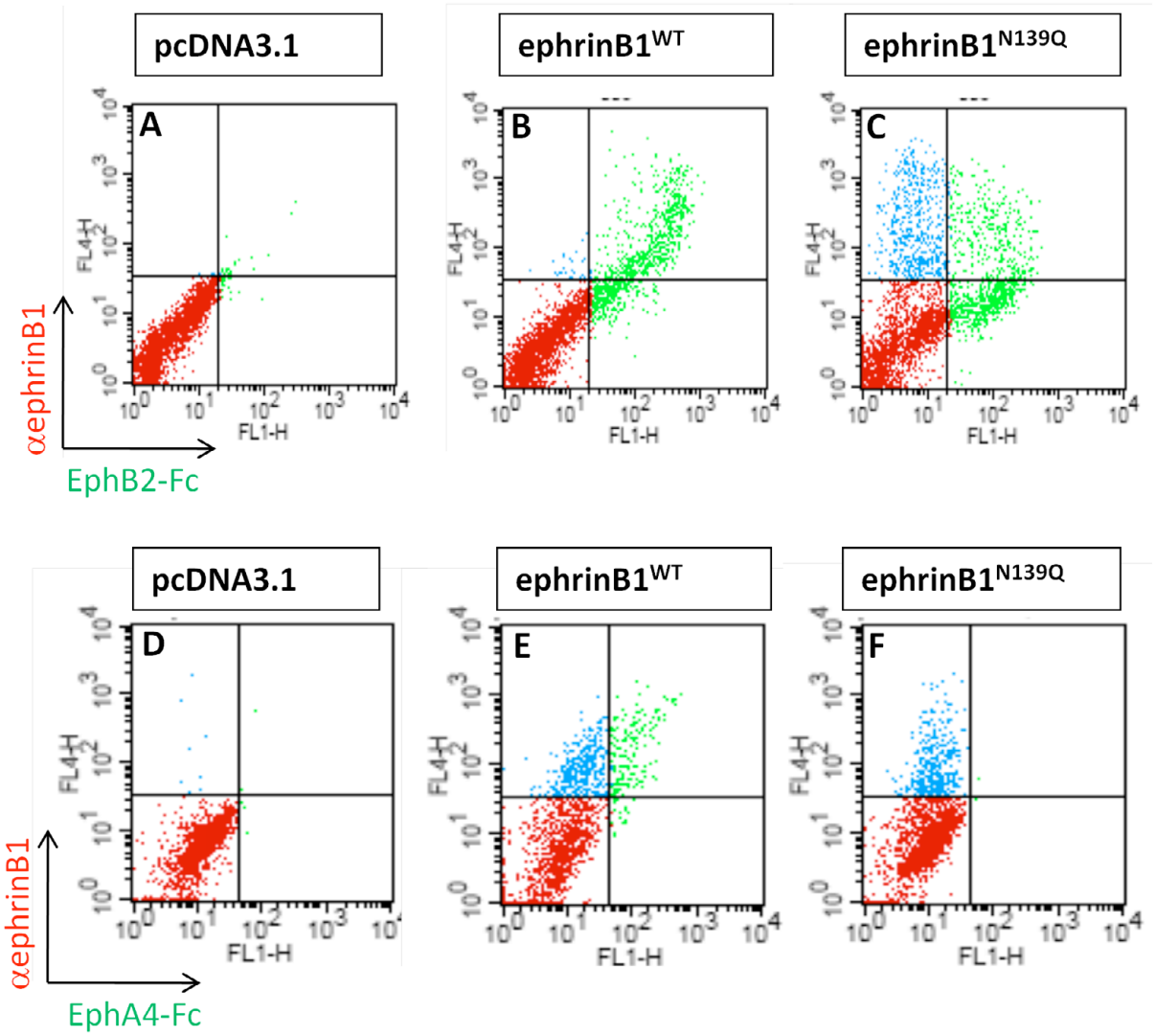

Fig. S8. EphB2 is the preferred receptor for ephrin B1. (**A-F**) FACS analysis demonstrates that the majority of cells expressing ephrin-B1^{WT} bind EphB2-Fc (B) but only a fraction bind EphA4-Fc (E). EphB2-Fc binds less efficiently to cells expressing a form of ephrin B1 mutated on a putative N-glycosylation site (N139Q) (C) while this mutation completely abolishes binding of EphA4-Fc (F). These results indicate that EphB2 is a preferred receptor for ephrin B1 compared with EphA4.

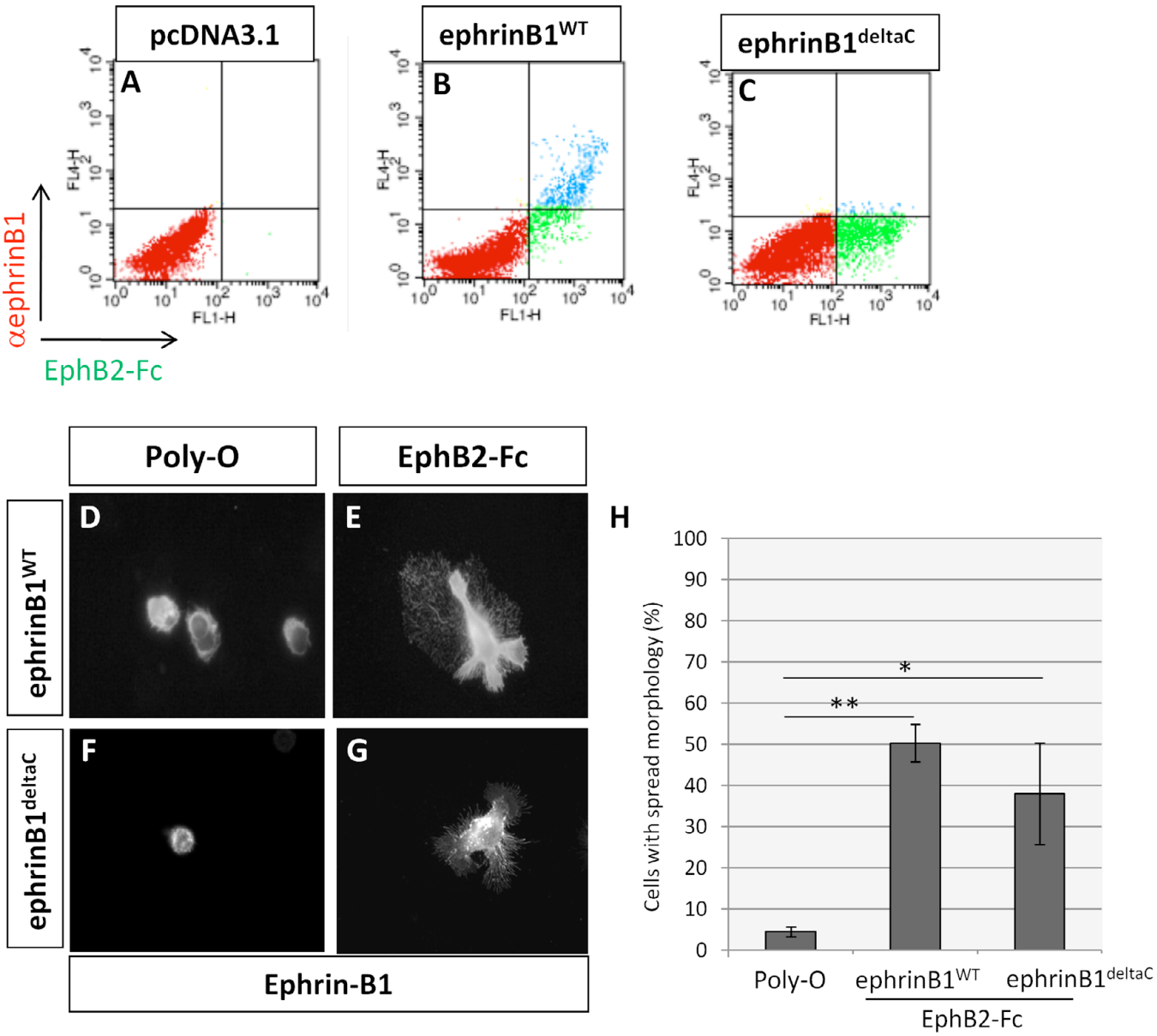

Fig. S9. A truncated form of ephrin B1 lacking the cytoplasmic domain induces cell adhesion and spreading. (**A-C**) Ephrin-B1^{deltaC} corresponds to amino acids 1-268 of mouse ephrin B1. FACS analysis demonstrate that similar to ephrin-B1^{WT} , ephrin-B1^{deltaC} binds EphB2 (FL1-H channel); however, ephrin-B1^{delatC} is not detected by C18 (FL4-H channel). These results indicate that ephrin-B1^{delatC} is expressed at the membrane and does not possess a cytoplasmic tail. (**D-G**) HeLa cells were transfected either with ephrin-B1^{WT} (D,E) or ephrin-B1^{deltaC} (F,G) and plated for 3 hours on glass coverslips coated with either poly-ornithine or poly-ornithine+EphB2-Fc. Cells were fixed and stained with an antibody directed against the extracellular domain of ephrin-B1 (R&D Systems). (**H**) Quantification of cell spreading. Statistical analysis was performed with a Student's *t*-test. $^{**}P<0.01$; $^{*}P<0.05$. Error bars represent s.d.

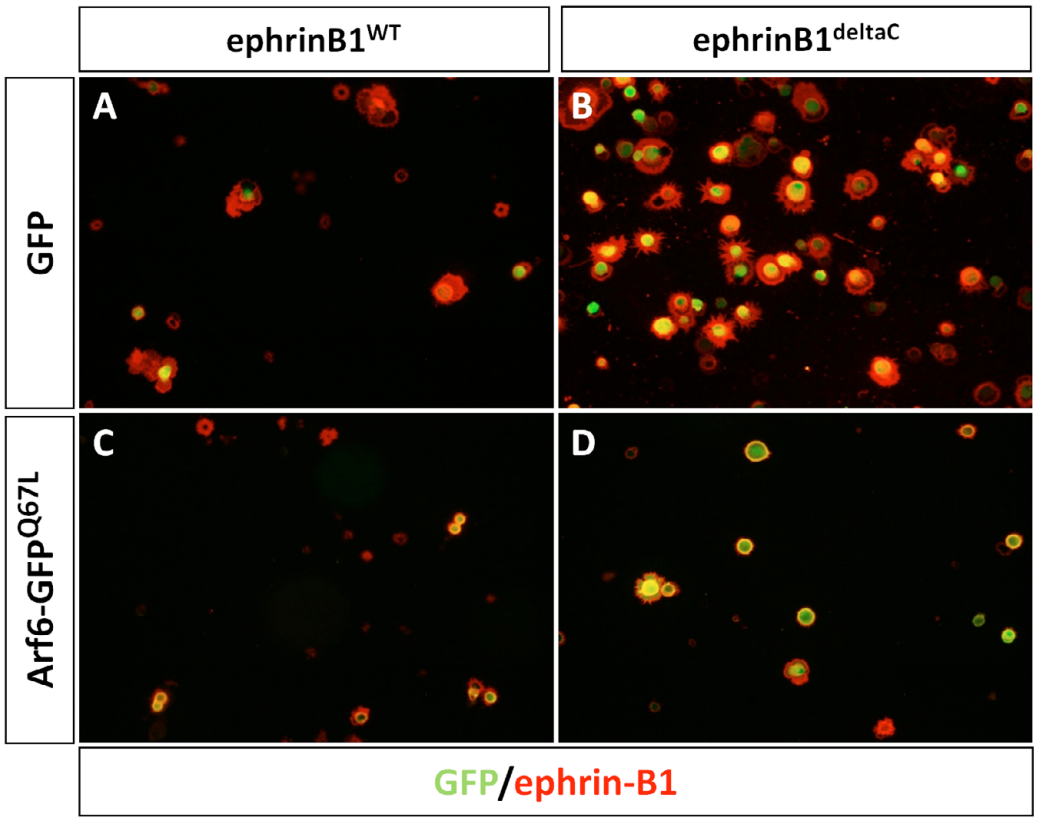

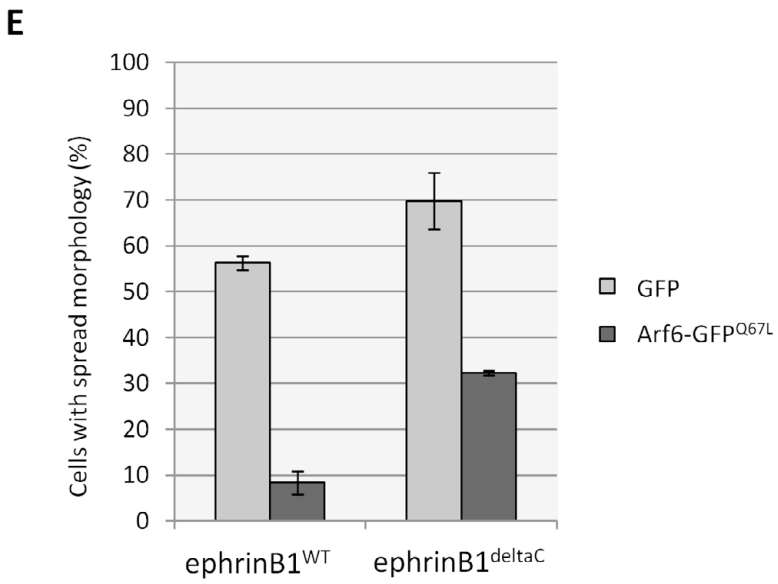

Fig. S10. Ephrin B1-induced cell spreading is blocked by Arf6^{Q67L}. (**A-D**) HeLa cells transfected either with ephrin B1^{WT} or ephrin B1^{deltaC} and co-transfected with either GFP or ARF6-GFP^{Q67L} were plated on glass coverslips coated with poly-ornithine+EphB2-Fc and stained for ephrin B1. (**E**) Quantification of cell spreading on GFP+/ephrin-B1+ cells.